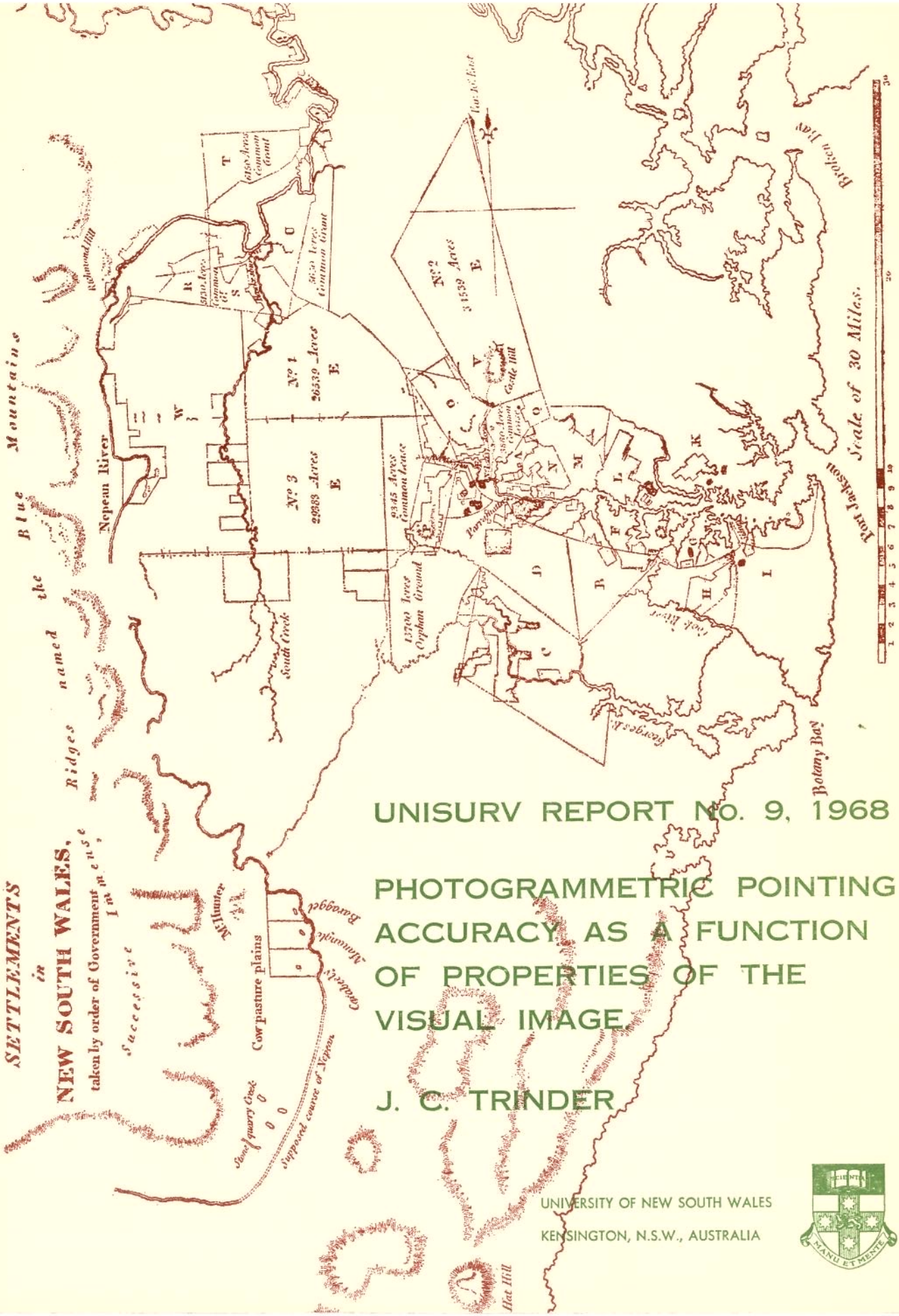


# UNISURV REPORT No. 9, 1968

# PHOTOGRAMMETRIC POINTING ACCURACY AS A FUNCTION OF PROPERTIES OF THE VISUAL IMAGE

J. C. TRINDER

UNIVERSITY OF NEW SOUTH WALES
KENSINGTON, N.S.W., AUSTRALIA

Reference to Districts.

A Northern Boundaries
B Liberty Plains
C Banks Town
D Parramatta
EEEE Ground reserved for Govt. purposes
F Concord
G Petersham
H Bulanaming
I Sydney
K Hunters Hills
L Eastern Farms
M Field of Mars
N Ponds
O Toongabbey
P Prospect
Q
R Richmond Hill
S Green Hills
T Phillip
U Nelson
V Castle Hill
W Evan

The cover map is a reproduction in part of a map noted as follows:

London: Published by John Booth, Duke Street, Portland Place, July 20th, 1810

Reproduced here by courtesy of The Mitchell Library, Sydney

UNISURV REPORT No. 9

# PHOTOGRAMMETRIC POINTING ACCURACY AS A FUNCTION OF PROPERTIES OF THE VISUAL IMAGE.

J.C. Trinder.

Received 10th February, 1968.

The Department of Surveying,
University of New South Wales,
P.O. Box 1,
Kensington, N.S.W. 2033
Australia.

# INDEX.


| | | Page. |
|---|---|---|
| 1. | EXPERIMENTAL DATA ON POINTING | |
| 1.1 | Introduction | 1 |
| 1.2 | Available data | 2 |
| 1.3 | Graphical Presentation of Data | 4 |
| 1.4 | Current Interpretation | 8 |
| 1.4.1 | Mach Phenomenon | 10 |
| 1.5 | Outline of Investigations and Definition of Terms | 12 |
| 2. | INVESTIGATIONS - CONVOLUTION OF ANNULUS AND SPREAD FUNCTION OF THE VISUAL SYSTEM | |
| 2.1 | Spread Functions | 13 |
| 2.2 | Spread Function of the Visual System | 15 |
| 2.3 | Convolution of Annulus and Spread Function of the visual System | 19 |
| 2.3.1 | Introduction | 19 |
| 2.3.2 | Convolution of the Three-Dimensional Point Spread Function and Annulus Profiles | 22 |
| 2.3.3 | Convolution of Line Element and Line Spread Function | 26 |
| 2.4 | Interpretation of Convolved Curves | 26 |
| 2.4.1 | Maximum Luminance Levels | 26 |
| 2.4.2 | Slopes of the Profiles | 30 |
| 2.4.3 | Widths of the Luminance Profiles | 32 |
| 3. | DISCUSSION OF RESULTS OF CONVOLUTION | |
| 3.1.1 | Shapes of Convolved Annulus | 38 |
| 3.1.2 | Pointing Accuracy as a Function of Slopes and Maximum Values of the Radiance Profile | 41 |
| 3.1.3 | Pointing Accuracy as a Function of Width Discrimination for Larger Annuli | 44 |
| 3.2 | Discussion of Results based on Dark Adaptation | 48 |
| 4. | SUMMARY | 48 |
| 5. | FURTHER APPLICATION. | 50 |
| 6. | CONCLUSIONS | 50 |
| | Appendix A | 52 |
| | Appendix B | 54 |
| | Appendix C | 56 |
| | Bibliography | 63 |
| | Biographical Notes | 65 |

SUMMARY: Investigations into pointing to sharp, high and low contrast targets in photogrammetry have revealed that pointing accuracies are linearly dependent on the width of the annulus or "edge ribbon", around the measuring mark for large annuli. For very small annuli, however, the relationship is more complex. While no firm explanations have as yet been put forward which explain the processes involved, the Mach phenomena has been proposed as a contributing factor. Based on the method developed by the author in a previous work, a study of images actually seen by the visual system has been carried out, in an effort to explain pointing accuracies via this image, rather than by purely geometric properties in the annulus.

The work combines physiological data on the visual system with current data on pointing by other scientists. The spread function, which is the spreading effect of the visual system on very small objects, is combined by convolution with the annulus using computational methods. Analysis of the image seen by the visual system has led to the postulation of simple criteria on which pointing to small annuli is based. It is maintained that a similar analysis on pointing to blurred targets will reveal criteria consistent with those deduced from sharp targets.

# 1. EXPERIMENTAL DATA ON POINTING.

## 1.1. Introduction.

The measurement of photograph or model coordinates in aerial triangulation involves pointing to photographic targets with a measuring mark. Pointing is, in effect, the task of centring a dark circular measuring mark on a bright, roughly circular target. Such targets can be either photographed premarked ground points, or artificial pricked points in the emulsion of the photograph. Under magnification, the edges of these targets appear blurred and ill-defined. Each step in the formation of the photographed points adds to the degradation in the quality of the image; some of the causes of degradation are atmospheric effects, image movement, imperfection in the camera lens, blurring effects of the emulsion, and granularity. The edges of pricked points are also ill-defined mainly due to physical factors in the formation of the points. A full study, including microphotographs of the point, has been made on pricked points by Hempenius (1964, 301-314). Pointing therefore cannot be considered as simply centring one sharp circular measuring mark on another. The additional factors of unsharp edges, variable contrast around the target, photographic grain and non-circular shape, all add to the difficulties in the pointing task, and therefore lower the accuracy.

In photogrammetric practice an estimate of accuracies in pointing to such targets using photogrammetric instruments with an

optical magnification of 10x is about 3-4$\mu$. In contrast with this figure stereocomparators are capable of pointing accuracies of 1-2 microns. On the other hand, the accuracy to which we should ultimately aim according to Schmid (1964) is 1 micron or better. Investigations aimed at closing the gap between the present and desired accuracies must analyse all aspects in aerial photography, measuring equipment and techniques, in order to develop a set of circumstances which will combine most efficiently to produce the best possible pointing accuracies.

Since the human eye is a basic factor in pointing, any research must incorporate investigations into its characteristics and capabilities. However, vision as such does not stop at the eye itself. Images projected onto the retina of the eye are transmitted to the brain where processing of size, shape, colour and density are carried out. Psychological factors may therefore also be involved (Hempenius, 1966a; 1966b).

## 1.2 Available Data.

Very few workers in the field of photogrammetry have adopted a fundamental approach to investigations on pointing in relation to the eye. However, O'Connor (1961) at the I.T.C. investigated monocular and stereoscopic pointing to sharp and blurred targets of different sizes using a number of different measuring marks. These experiments were made on Wild STK1 and Zeiss Pulfrich Stereocomparators. The investigations revealed that monocular pointing accuracy was linearly related to the width of the annulus between the edges of the target and

measuring mark, above a certain width of annulus, and constant below this level. The level of constant pointing accuracies became greater as the image quality deteriorated. The reader is referred to Hempenius (1964, 318) for full graphs of these investigations. They are plotted on a logarithmic scale with both the annulus, and pointing accuracies expressed in terms of angular subtense at the eye, in radian measure.

Subsequent experiments on the eye by O'Connor (1967) have been carried out on monocular pointing accuracies using special instrumentation and very sharp targets of high to low contrast. The instrument had no optical elements as did the stereocomparator, except two reflecting mirrors. This allowed him to use targets with edges of the utmost sharpness, since the instrument had a minimum effect on the quality of the image. In addition, the least count of this instrument was considerably lower than that of the stereocomparators used in the first experiment. The second series confirmed his belief that capabilities of the eye, at least in pointing to sharp targets, were considerably better than the least count of stereocomparators in general use.

Investigations in his second series were made firstly in terms of one variable - the annulus size or "edge ribbon" between the measuring mark and target, i.e. keeping contrast and image quality constant. Additional experiments were carried out substantiating the conclusions already reached in the first series, that measuring mark sizes are of minor importance in the determination of pointing accuracies (O'Connor

1962, 31; 1967, 7). After the analysis in terms of one variable - annulus width - a second variable, i.e. contrast of the target relative to its background, was added. Extension of O'Connor's investigations further could introduce additional variables, such as edge unsharpness and photographic grain.

The experiments so far have been carried out using ideal sharp targets which are far removed from those which occur in normal photogrammetric practice. However, the investigations have commenced from the simplest situation with a minimum of variables. Based on this work, additional variables may be added, thus bringing the investigations more into line with practical conditions.

The results of O'Connor's second series will be presented in the following section.

## 1.3 Graphical Presentation of Data.

In O'Connor's second study, extensive experimentation has been carried out on sharp targets of varying diameters using a number of different measuring mark (MM) diameters, at high, medium and low contrast. Results of these experiments are presented in Figs. 1 (a), 1 (b).

The curves have been plotted on logarithmic scales with the annulus or "edge ribbon" between MM and target on the abscissa scale, and pointing accuracy plotted on the ordinate scale. Each scale is

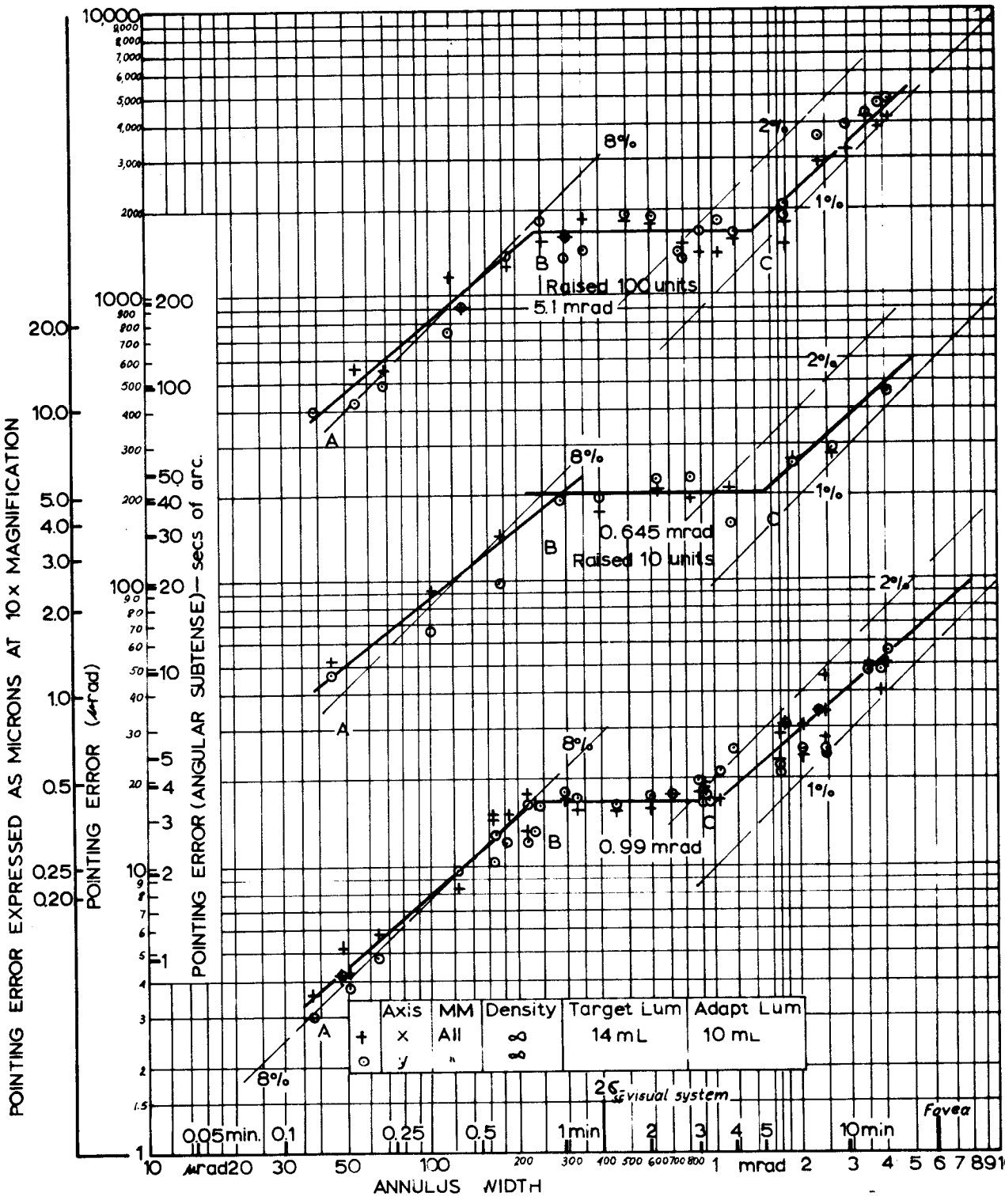


FIG. 1a POINTING ACCURACIES TO SHARP HIGH CONTRAST CIRCULAR TARGETS, USING 3MM's AS SHOWN, EXPRESSED IN TERMS OF THE ANNULUS BETWEEN TARGET AND MEASURING MARK. ANNULUS WIDTH AND POINTING ERROR HAVE BEEN EXPRESSED IN RADIAN MEASURE OF THE ANGULAR SUBTENSE AT THE EYE. POINTING ERRORS HAVE ALSO BEEN EXPRESSED IN TERMS OF MICRONS AT 10 x OPTICAL MAGNIFICATION.

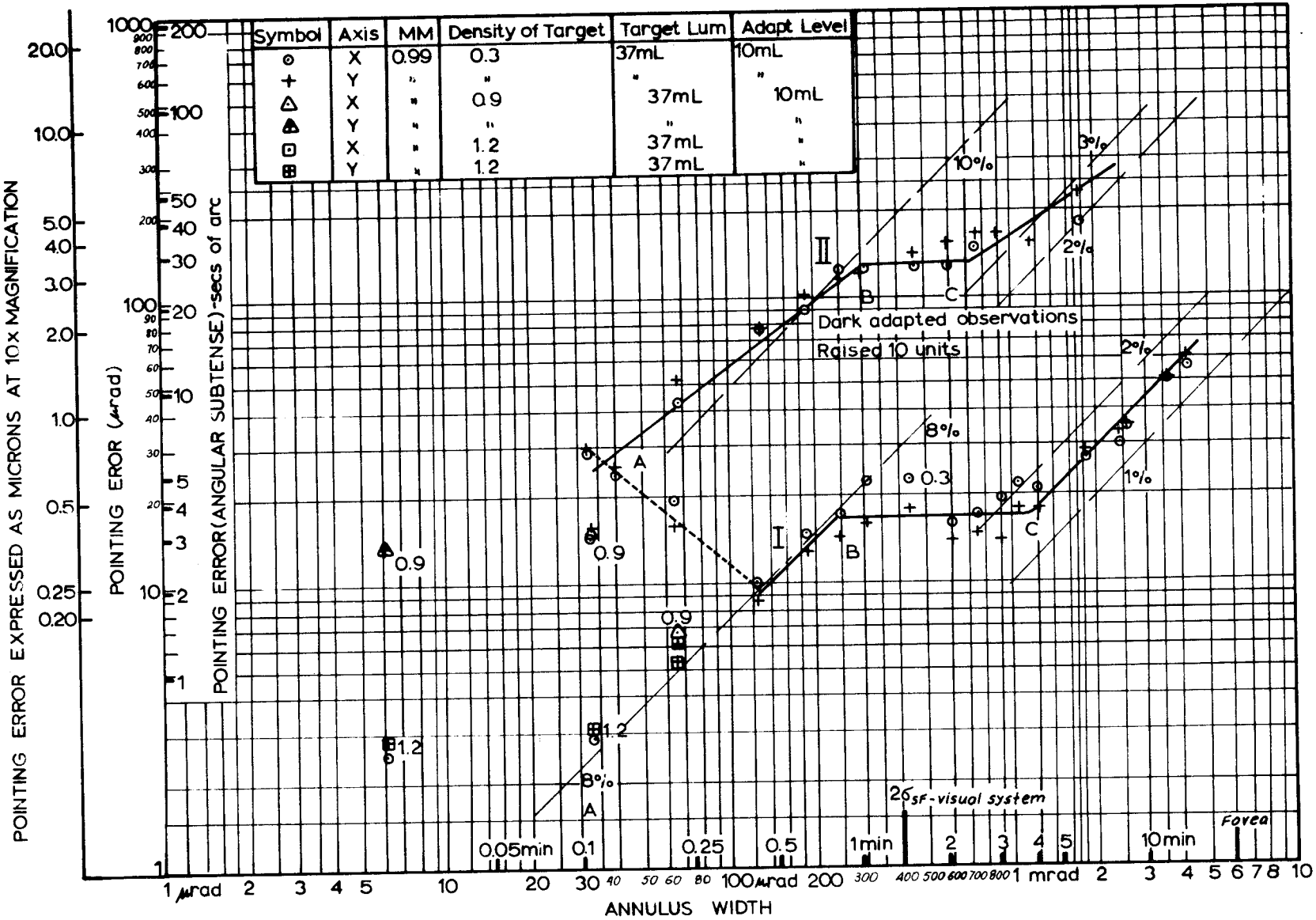


FIG. 1b POINTING ACCURACIES TO TARGETS OF BACKGROUND DENSITIES 0.3, 0.9 AND 1.2 (LOW TO MEDIUM CONTRAST), USING A MEASURING MARK OF 0.99 mrad, ARE EXPRESSED IN CURVE I. CURVE II GIVES THE POINTING ACCURACIES TO HIGH CONTRAST TARGETS WITH THE OBSERVER'S VISION ADAPTED TO DARKNESS

graduated in angular subtense expressed in radians. (1 min. of arc = 0.291 mrad = 291 μrad; 1 sec. of arc = 4.85 μrad.) The approximate size of the fovea and the approximate minimum width over which all small details are seen by the visual system (the spread function), have been added.

The curves in fig. 1(a) represent accuracies obtained in pointing in the x and y directions expressed as standard deviations, from repeated observations, using a MM of 0.99 mrad (3.41 min. of arc), 0.645 mrad (2.25 min. of arc) and 5.1 mrad (17.75 min. of arc). The x-direction is parallel to the eye-base, and the y-direction at right angles to it.

Results of pointing to low and medium contrast targets and high contrast targets based on dark adaptation have been presented in fig. 1 (b).

The interpolated curves in fig. 1 are those determined by Hempenius (1964) and also presented by the author in the previous work (1965, 6). The determination of an interpolated curve for the results is rather vague. O'Connor computed an exponential curve for points above an annulus of 250 μrad, and a straight line below this level. In fact for the present study, the shape of the interpolated curve is of minor importance. However, there seems some justification for the present figure since, as will be seen in Sec. 3, separate criteria have been deduced over each section of curve in fig. 1.

A full statistical investigation has been made by O'Connor. It has been established that pointing accuracies in the x and y directions

tended to differ in some cases for annulus widths less than 1.2 mrad (4 min. of arc) but differences were insignificant for annulus widths greater than 1.2 mrad. For the present study, curves in fig. 1 have been interpolated using both x and y observations. On viewing the results, there are no large systematic differences between x and y errors.

Observations were carried out by several observers, both experienced and inexperienced. These tended to differ significantly, although the same pattern resulted. For this reason, only the observations by O'Connor will be treated in this paper. It is believed that these differences are due to personal factors, and not to any variations in the basic criteria used in pointing.

## 1.4 Current Interpretation.

Pointing accuracies to high contrast targets seem to follow a complex relationship with annulus width, but are basically independent of MM size. As presented in fig. 1 (a), below point B pointing accuracies increase steeply following an approximate 8 $^{o}/o$ relationship. Between B and C, pointing accuracies appeared to be constant, and above point C accuracies slowly increased, following approximately a 1-2 $^{o}/o$ relationship with annulus width. Pointing accuracies to low contrast targets followed the same pattern as for high contrast targets, except for annuli less than 250 $\mu$rad where at a certain point, depending on the density of the background, accuracies decreased sharply.

The level at which pointing accuracies were constant in these experiments, was 17-20 $\mu$rad for the x and y directions. The constant level for the previous experiments by O'Connor (1961) varied from 42 $\mu$rad to 120 $\mu$rad, depending on the image quality of the targets. It is apparent that increased blurring at the edges of the targets, causes higher pointing errors.

O'Connor (1961) has indicated that for annuli in the range greater than 1 mrad, where accuracies tend to follow the 1-2$^{o}$/o relationship, Weber's Law applies. Weber's Law is used in the study of differential sensitivity of human senses (or limen), and its general form states that a sensation increment is proportional to the ratio of

$$\frac{\text{just noticeable stimulus}}{\text{total stimulus.}}$$

O'Connor has indicated values for the visual system varying from 1$^{o}$/o to 2$^{o}$/o. These results are generally based on mean variations of settings in equating lengths (and not standard deviations), with the provision that lengths must not be too long or too short. O'Connor has further proved that it is possible to equate areas or widths on each side of the MM to Weber's Law. Stated in terms of pointing, Weber's Law can be rewritten as

$$\frac{\text{Pointing error } ^{o}/o}{\text{Annulus Subtense}} \quad .$$

In his second publication, O'Connor proposed that pointing accuracies for the small annuli, were dependent on adjacency effects

at the edges of the targets. Neural correlates appeared to be a contributing factor in pointing accuracy rather than strict geometric properties of the targets. He further concluded that the Mach phenomenon could be a significant factor contributing to adjacency effects. However in the experiments to sharp circular targets to date, Mach bands have not been consciously observed, although the possibility of their existence subliminally is not precluded. It was noted that a pronounced contrast at the border was observed for the lowest contrast targets.

Although investigations in this paper are not based on the Mach phenomenon, a brief description will follow.

### 1.4.1 Mach Phenomenon.

As explained by O'Connor (1967, 41) when a one dimensional luminance distribution is viewed by an observer (e.g. parallel bright and dark areas separated by a transitional area), a bright band apparently brighter than the original pattern is seen along the edge of the bright region. Also, along the edge of the dark region, a dark band is seen, which itself is darker than the original pattern. These bands are called Mach bands. A number of investigations have been carried out on the width and intensity of these bands which are described by Ratliff (1965, Chap. 2).

In pointing to small targets the size of the luminance distributions can be described as microscopic - in the order of 1 mrad. Experiments on this type of profile have been carried out by Charman and Watrasiewicz (1964) and Watrasiewicz (1966). Their investigations found the same bright and dark bands, but in addition, at least one smaller secondary dark band adjacent to the luminance intensity change. Also, as the contrast between the light and dark areas decreased, the secondary bands disappeared, but the contrast of the observed pattern became accentuated. According to Watrasiewicz (1966, 501) at a contrast similar to that in the observation to targets of 0.3 background density, this accentuation was as much as two-fold. Such an accentuation in the apparent contrast, as mentioned previously, was noted by O'Connor in the observations to low contrast targets. It is also noteworthy that Watrasiewicz found that the Mach bands disappear completely for retinal illuminances below 15 trolands*. This is equivalent to a target luminance of approximately 0.7 mL, for a pupil diameter of 3 mm, ignoring the Stiles-Crawford effect.

---

* Retinal illuminance is defined as L.S. trolands, Graham (1965, 11-13) where L is the luminance of the stimulus in candelas/sq. m., (3.1 candelas/sq.m = 1 mL), and S is the area of the pupil in mm$^2$. A number of difficulties arise in the use of retinal illuminances:-

(i) amount of light at the retina is not constant with wavelength;
(ii) area of pupil can vary for different observers;
(iii) light entering the marginal areas of the pupil is less effective to retinal stimulation than light entering the centre of the pupil.

This is known as the Stiles-Crawford effect. The loss in effective illuminance for a 3 mm diameter pupil is about 5$^{o}$/o Walsh (1953, 60) Because of the indefinite nature of the retinal illuminance, no attempt is made to correct for this difference.

## 1.5 Outline of Investigations and Definition of Terms.

Proposals on edge effects have resulted in no firm conclusions. Investigations in this paper will therefore treat the problem from a different point of view. The image of the annulus as seen by the visual system will be investigated for the purposes of finding some correlation between this image - the image, in fact, used by the observer for pointing - and the curves of fig. 1. No further pointing experiments will be carried out. Instead, pointing accuracies derived by O'Connor as in fig. 1 will be combined with physiological data on the visual system.

The term "brightness" in this study will be replaced by the physical terms "radiance" and "luminance" and brightness will be restricted to the visual sensation of a luminance stimulus. If the pattern of brightness over an object either reflected or transmitted, e.g. a line, is measured by a light sensing instrument, the profile resulting is termed a luminance or intensity profile. The abscissa scale refers to the position x on the object, while the ordinate scale, the intensity readings either in relative or absolute units, for each position x, see fig. 2.

The visual system is capable of discerning differences in widths or differences in light intensity or luminance within an image, i.e. differences in width or differences in levels of intensity in an intensity profile. The shape of the intensity profile as seen by the visual system therefore will be resolved in terms of width and intensity distributions.

For this, the spread function, which is the blurring effect of the visual system, is combined by convolution with the luminance profile of the annulus to derive the luminance profile seen by the visual system, in the following section.

Before proceeding, however, the difficulties encountered in resolving the width of the annulus actually seen by the visual system must be mentioned. For instance, looking at the line in Fig. 2, where should we measure the width of this line, and at what level on the profile is this width measured? A limited amount of research has been carried out on this question. Reference will be made to these investigations in Section 2.4.2. Width determination ideally could be incorporated as part of the experiment. However, it was not carried out as part of O'Connor's experiments. It is probable that a particular level or contour on the luminance profile, depending on the adaptation level, is used for width determination. At this stage, such a level is unknown. For the purposes of these investigations two criteria have been adopted. Although these criteria may not be correct, it is felt that errors introduced will not influence conclusions appreciably.

## 2. INVESTIGATIONS - CONVOLUTION OF ANNULUS AND SPREAD FUNCTION OF VISUAL SYSTEM.

### 2.1 Spread Functions.

All image-forming systems cause a spread or "loss in edge sharpness" and a blurring of small details in an image, depending on

the design and fabrication of the imaging system. This spread, which is formulated by a spread function, is the resulting intensity or luminance profile across the image formed by the optical system, of a very small detail, either a line or a point. The resulting functions, i.e. line spread function (LSF) and point spread function (PSF) are the basic functions which can be used to determine the projected images of an object of any shape or size. Such functions characterize the standard of imaging quality of the system.

The line spread function of a lens for instance, can be found by scanning the image formed by the lens, of a very thin sharp line with a slit much narrower than the line itself. A measurement of the light passing through the slit at each successive position gives the resultant LSF, similar to the profile in fig. 2. In a similar manner, the PSF can also be determined. If the image point being scanned is asymmetric, a number of scans in different directions may be necessary. The graphical representation of the PSF must be in 3 dimensions. Alternatively it can be represented by 'contours' in a 2-dimensional diagram.

The characteristics of the optical system of the eye can also be described by a LSF and a PSF. However, spread functions derived for the eye should apply to the complete visual system since the visual

process involves not only the optics of the eye, but also the interpretation by the brain and neural processing* between the eye and brain. Therefore, the word "eye" in the following will be replaced by the words "visual system."

2.2 Spread function of the Visual System.

Early investigations made on the visual system by Krauskopf (1962), Westheimer and Campbell (1962) and Röhler (1962) to find its SF only explored characteristics of the optical system of the eye itself without considering the function of neural processing in the cortical or other centres of the visual system. As stated by Gubisch (1967, 407) results from such measurements indicated a much poorer performance of the visual system, than was obtained by acuity tests. This led some physiologists to believe that image sharpening mechanisms accounted for the difference. The previous work by the author (1965) was based on a PSF computed as a Gaussian approximation from the PSF determined by Röhler (1962).

However, subsequent investigations carried out by Patel (1966), Gubisch (1967), Fry (1965) and others, indicate a higher imaging quality than that formerly determined. Patel's investigations which have produced SF's for the total visual system present curves for the LSF of the visual system, for a number of retinal illuminances,

* It is not intended to discuss the complex processing of the visual information between the eye and brain. A very comprehensive description of this section is given by O'Connor (1967, Appendix A)

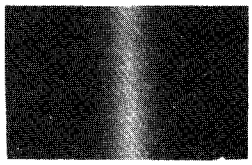

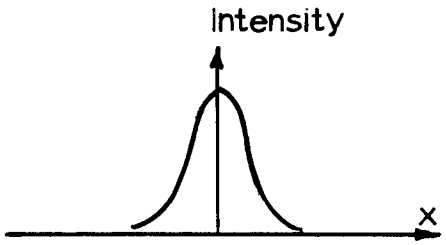


FIG. 2 BLURRED IMAGE WITH ITS INTENSITY PROFILE.

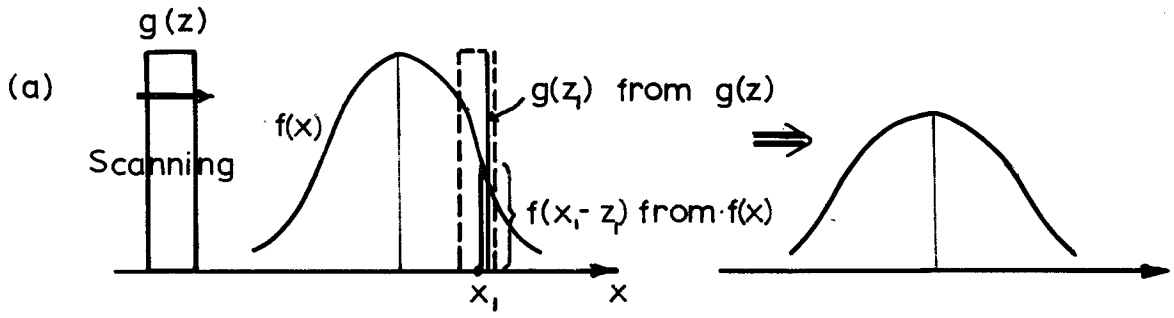


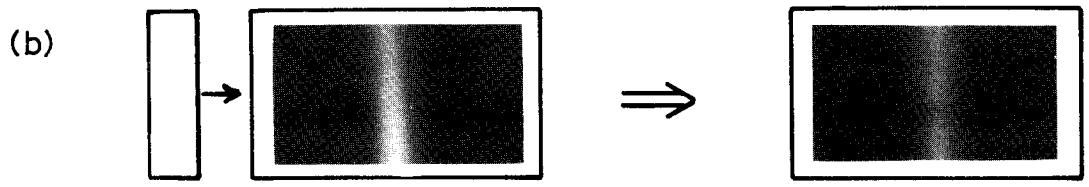


FIG. 3 CONVOLUTION BY SCANNING
(a) MATHEMATICALLY.
(b) USING LUMINANCE PATTERN AND LIGHT SENSING INSTRUMENT.

while Gubisch has computed the PSF for 8 pupil diameters. A significant feature of these investigations on the visual system is that imaging quality changes with retinal illuminance. This feature is noticeably different from a purely physical lens system which is independent of luminance over a wide range of intensities. In Patel's publication an interesting comparison is given of the LSF of the optics of the eye derived by Westheimer and Campbell, and Krauskopf, with that of the total visual system.

Gubisch determined the PSF for the optical system for a number of pupil diameters, for the purposes of computing the sizes of images on the retina of small test targets including annuli, and also for determining glare in the retinal image. O'Connor's (1967) adaptation level was based on a screen with a luminance of 10 milli-Lamberts (mL). This would result in a pupil diameter according to Walsh (1953, 55) of approximately 3 mm. The instrument used in the experiment had an artificial pupil of 4mm diameter. The PSF for a 3 mm pupil according to Gubisch follows closely a gaussian curve whose $2\sigma$-width is 200 $\mu$rad. It has been found that this PSF compared well with that determined by Fry (1965).

Patel found the LSF to have a $2\sigma$-width of approximately 400 $\mu$rad for a comparable pupil size. It has been proved (Trinder, 1965) that the LSF can be derived from the PSF by dividing a line into a number of points each of which is spread by the PSF. (See also Section 2.3.2) Using a gaussian PSF, the $2\sigma$-width of the resulting LSF will equal that of the PSF.

The $2\sigma$-value of Patel for the total visual system can therefore be compared with that of Gubisch and Fry for the optical system.

Values of the PSF given above represent those strictly of the visual system. However, the instrument used by O'Connor incorporates two reflections on mirrors before projection into the eye. Consequently the combined imaging quality of the instrument and visual system may well be slightly lower than that of the pure visual system. It was felt, therefore, that a gaussian PSF with a $2\sigma$-width of 400 $\mu$rad would be a suitable value for the investigations.

The equations for the PSF and LSF therefore are respectively:-

$f(x, y) = \exp\left\{-(x^2+y^2)/80,000\right\}$ , where x and y, in $\mu$rad

$f(x) = \exp\left\{-x^2/80,000\right\}$ represent the coordinates on the point or line

A basic assumption made in using this approach is that the spread function is invariant over the small variation in luminance levels used in these investigations. The results of Patel and Gubisch indicate that for large variations in luminance this is not the case. In addition, the visual system is assumed to respond linearly to intensity variations. There are reasons for believing that this may not be the case for large differences in intensity, (O'Connor 1962, 50) but any errors caused by this assumption should be insignificant for the present study. Such assumptions were made by Lowry and De Palma (1961) and Patel (1966) in their investigations on the visual system. Good agreement between their values is an indirect justification of the above assumptions.

The radiance profile of the annulus actually seen by the visual system is derived by convolving the luminance profile of the annulus with the PSF in sec. 2.3.2. *

## 2.3 Convolution of Annulus and Spread Function of the Visual System.

### 2.3.1 Introduction.

When a lens forms an image, for instance, of a line with a given intensity profile, the quality of the resulting image will not be as good as that of the object. All imaging systems cause such a loss in quality of the image. This is manifested in an intensity profile of the image, the slopes of which are not as steep as those of the original profile, and maximum intensity probably reduced. When viewing the line, this would be interpreted as a greater blurring than the line had previously, as well as a loss in brightness. This process can be formulated as follows: the object intensity profile is affected by the imaging quality of the lens - described by the spread function of the lens - to produce the image intensity profile. The process of combining the object intensity profile and the SF in mathematical terms is called Convolution. Convolution is described (Jennison, 1961, 6) as "the operation whereby a structure under observation is smeared or spread out by the response or resolution of an instrument or mathematical operation." Here, the structure is the intensity profile of the object, the "instrument", the lens.

* Although the PSF above is said to apply to the total visual system, it is not held that it completely covers all neural effects particularly lateral inhibition. However since these effects have not been accurately formulated, the above value will be adopted as a close approximation to the correct value of the PSF for the total visual system.

The general formula for the convolution of a two dimensional object and line spread function is:-

$$h(x) = \int_{-\infty}^{+\infty} f(x-z).g(z).dz \quad \text{(Jennison, 1961, 47)} \quad \ldots\ldots(1)$$

where h(x) is the ordinate at point x after convolution, and f(x) and g(z) represent the two functions to be convolved. Each element dz of the function g(z), must be multiplied by the relevant value of f(x) i.e. f(x-z), and the total effects added.

Convolution can also be considered as the function f(x) being scanned mathematically by the function g(z) (Hempenius, 1964), (Jennison, 1961, 4-9), in the same manner as a slit scans the luminance pattern of an object. At each position x of the scanning function g(z), every element of g(z) is multiplied by the corresponding element of f(x) i.e. f(x-z). The addition of results after multiplication of corresponding elements, for all coordinates z, produces the ordinate of h(x).

The scanning can be carried out physically as well as mathematically. Fig. 3(a) shows the scanning of intensity profiles, with the associated multiplication and addition. Fig. 3(b) demonstrates the scanning of a slit in close contact with the luminance pattern. Summation is carried out here because the total light passing through the width of the slit is measured at each slit position. Each procedure gives identical results.

The physical approach of scanning must be used carefully, because convolution is not only addition. Formula (1) shows that the

relevant values of each function must be multiplied before addition is carried out. When one of the functions has a simple intensity profile, as for instance the slit, the multiplication factor of the slit is constant throughout, and therefore no multiplication is required if only relative values are needed. If however, the convolution involves two functions similar to f(x), the physical scanning must be carried out using a slit of variable transmittance, e.g. a transmittance profile similar to that of the blurred line. Provided this is done, the convolution will be correct.

One feature that should not be forgotten, is that either function can be used as the scanner. Logically it can be seen from fig. 3, that the same result must be obtained whether g(z) or f(x) is used as the scanning function, (Hempenius, 1965) (see also Trinder 1965).

To maintain constant energy before and after convolution, the ordinates h(x) must be normalized. This is done by dividing h(x) by the area under the original scanned function f(x). In the following discussion, only relative differences are required, and therefore the coordinates are not normalized.

A number of techniques are available for carrying out convolution in the more complex cases, particularly those which involve the PSF, namely, analogue, graphical and computational methods, (Trinder, 1965). The computational methods used in these investigations based on the scanning concept, will be explained in the following section.

2.3.2 Convolution of the Three-Dimensional PSF and Annulus. Profiles. ("PSF method").

Extension of the formula (1) to the 3-dimensional case is as follows:-

$$k(x, y) = \int_{-\infty}^{+\infty} \int_{-\infty}^{+\infty} f(x-z, y-w)g(z, w)\, dzdw \quad \ldots\ldots\ldots\ldots\ldots (2)$$

Mathematical integration of this formula for the functions in hand proved to be more difficult than the scanning technique.

The profiles of annulus and PSF are shown in fig. 4. The intensity profile across AA, can be determined, by scanning AA by the PSF. At each scanning position of the PSF, the products of the ordinate g(x, y) of the PSF, are multiplied by the corresponding ordinate of the annulus f(z, w) over the entire annulus. The sum of all products then gives the ordinate for the scanning position on AA.

The annulus was divided into small segments approximately 5 $\mu$rad square. Because of the simplicity of f(z, w), where the relative ordinate is either 1 or 0, the computation amounted to evaluating the ordinate of the PSF for each small segment using the distance from scanning point to the segment centre. Summation of these ordinates then gave the required value for each point along AA.

The influence of each element is proportional to its volume, by the law of conservation of energy, i.e. the volume of each element after spreading must equal the volume of the element before spreading. The correct relative influence of each element was therefore obtained by multiplying the evaluated ordinate of the PSF by the volume of the

$g(z,w)=1$ if polar coord $r_1 < r < r_2$

$g(z,w)=0$ if polar coord $r_1 > r > r_2$

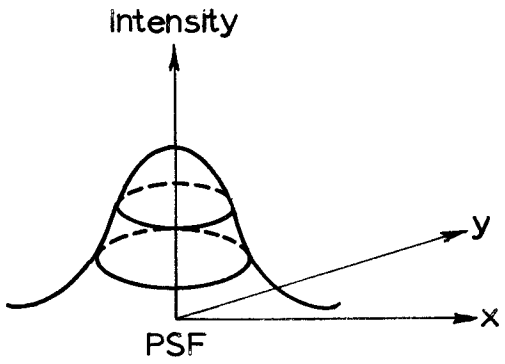


$$f(x,y)=\exp\left[-(x^2+y^2)/2\sigma^2\right]$$

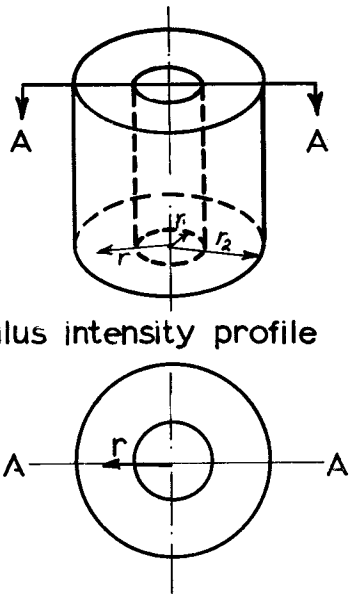


Annulus intensity profile

FIG. 4 PICTORIAL REPRESENTATION OF PSF, $f(x,y)$ AND ANNULUS INTENSITY PROFILE $g(z,w)$ TOGETHER WITH RESULT AFTER CONVOLUTION.

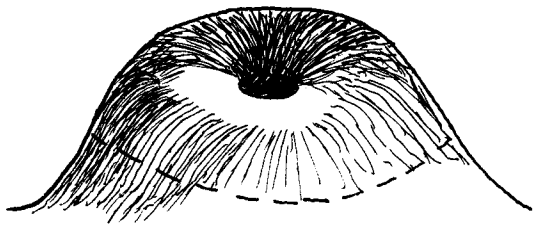

element.

The size of the elements, although finite, proved to be sufficiently small. Investigations were carried out to find a practical sized element. The use of elements approximately 5 $\mu$rad square introduced errors of less than $1^{o}/o$, which was acceptably low for these investigations.

In the computer program, provision was made to introduce small displacements of the MM on the target, along the line AA, so that variations in the intensity profile could be observed as the MM is varied. Displacements equal to the errors in pointing were introduced so that just perceptible changes in the radiance profile for varying annulus widths could be determined.

Output from the convolution were ordinate values of the convolved curve at intervals of 50 $\mu$rad along AA. This interval was sufficient for the interpolation of maximum values and widths as mentioned in Sec. 2.4.

2.3.2(a) Medium and Low Contrast Targets.

Convolutions of the targets with background densities of 0.3, 0.9 and 1.2 were carried out in a similar manner, but the profile had to be divided into 2 sections, and the effect of one subtracted from the effect of the other. This was the technique used by Gubisch(1967, 412) to determine the profile of an annulus. (See Appendix B for full details.)

The profile was divided as shown in fig. 5.

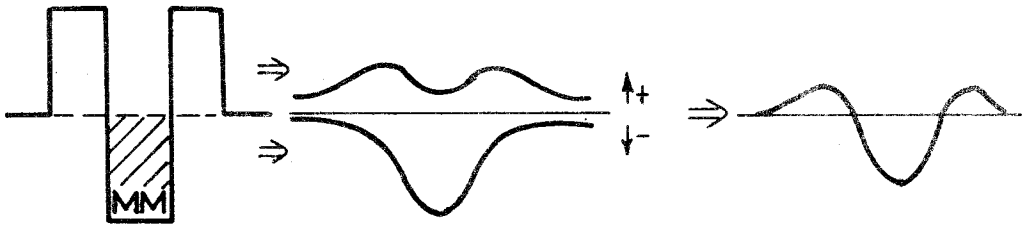


FIG. 5 DIVISION OF INTENSITY PROFILE INTO 2 SECTIONS, EACH OF WHICH IS CONVOLVED SEPARATELY, AND THEN ADDED.

The section above the background luminance level was convolved in the usual manner, i.e. as if the annulus had an infinite background density. The MM section below the background level was then convolved. This had a negative effect, that is an effect which caused a decrease in luminance level. Subtraction, therefore, gave the resulting profile which was asymmetric.

Cross-section graphs of the convolution have been presented in Appendix C for the three measuring marks at a number of annulus widths. In addition, results for the medium and low contrast targets (MM=0.99 mrad) have been presented in Appendix C.

Interpretation of these convolutions will follow. However, firstly the more simple convolution of the LSF and linear elements of different widths will be carried out. This is particularly applicable to annuli using MM of 5.1 mrad where the annulus tends to a linear object, for short intervals.

2.3.3 Convolution of Line Element and LSF ("LSF Method").

The computation was carried out using formula (1)

where $f(x) = \exp(-\frac{1}{2}x^2/\sigma^2)$ for $-\infty < x < +\infty$

$g(z) = 1$ for $-c < z < +c$

$= 0$ for $-c > z > +c$

and the annulus width is 2c. See fig. 3(a).

Annulus widths were chosen to represent widths when the MM was correctly centred and when the error in centering equalled those in fig. 1. Sample curves from this convolution have been presented in Fig. 6.

In the following section, the results from this convolution, and those using the PSF have been interpreted in terms of maximum levels of luminance, slopes of the sides and widths of the intensity profiles.

## 2.4 INTERPRETATION OF CONVOLVED CURVES.

### 2.4.1 Maximum Luminance Levels.

#### 2.4.1(a). High Contrast Targets.

Fig. 7 indicates the variations in maximum intensity on each side of the MM, for displacements of the MM equal to errors in fig. 1. They are expressed as percentages of the maximum intensity, ($I_{max}$), when the MM is correctly centred on the ordinate scale, with annulus width as abscissa.

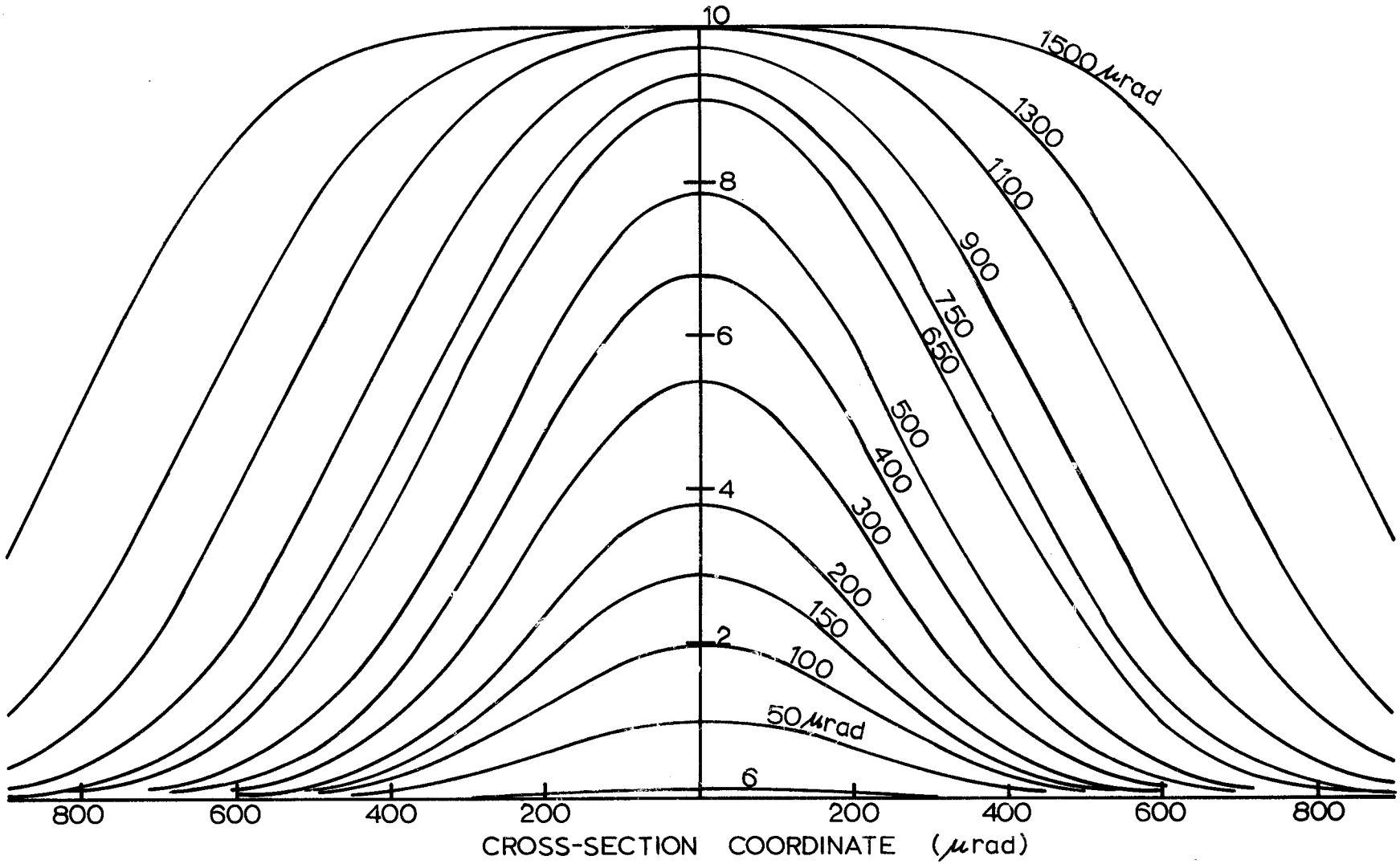


FIG. 6 RESULT OF CONVOLUTIONS OF LINE ELEMENT AND LSF. THE ORDINATE SCALE IS EXPRESSED IN ARBITRARY UNITS OF THE INTENSITY PROFILE. THE ABSCISSA SCALE RECORDS THE DISTANCE FROM THE CENTRE OF THE LINE ELEMENT. THE WIDTH OF THE ORIGINAL LINE ELEMENT HAS BEEN MARKED ON THE RELEVANT CURVES.

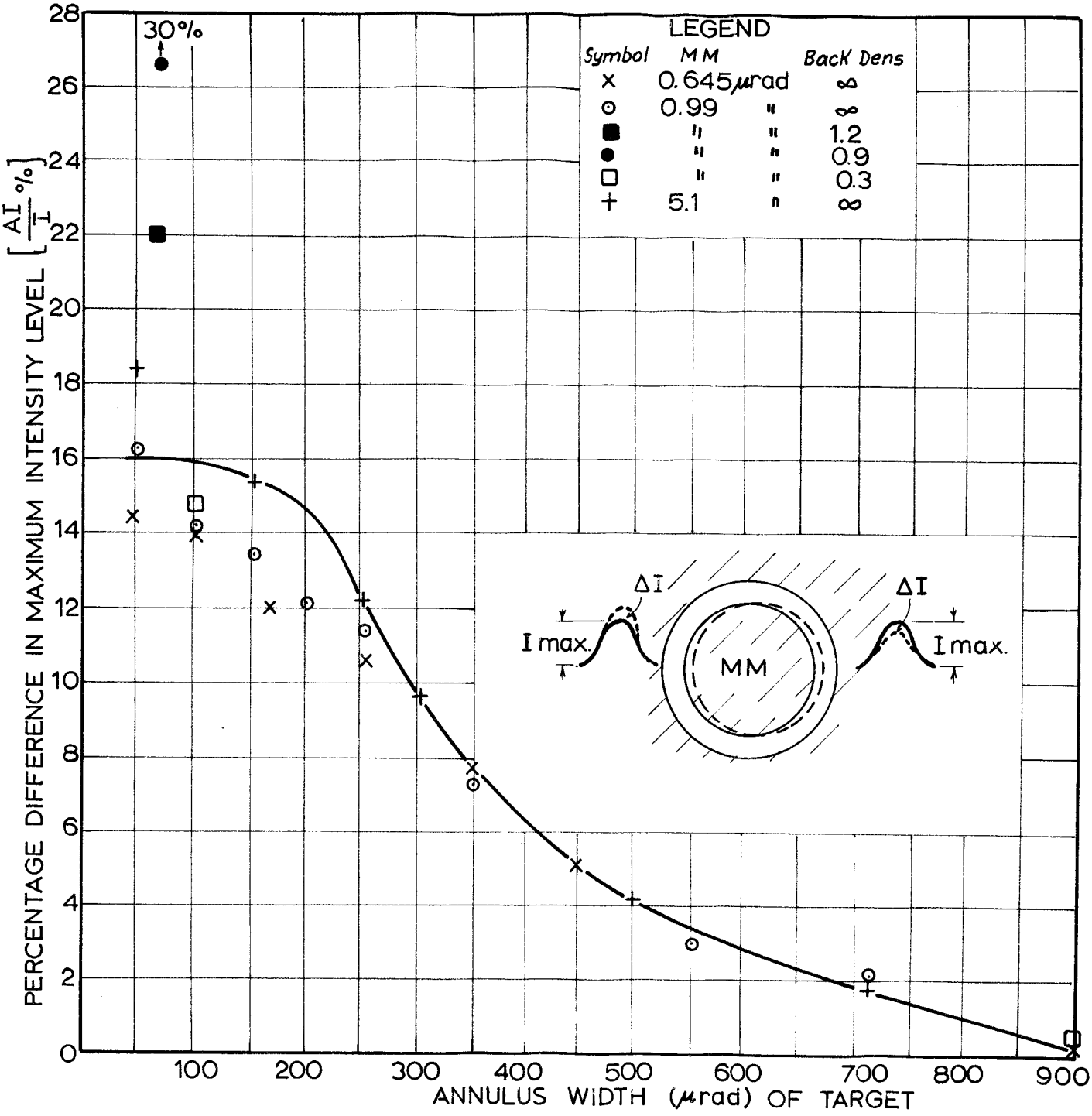


FIG. 7 THE RELATION BETWEEN PERCENTAGE CHANGE IN INTENSITIES OF EACH ANNULUS IN THE CONVOLVED PROFILE, AGAINST ANNULUS WIDTH. THE CURVE HAS BEEN COMPUTED BY THE LSF METHOD. THE RESULTS BY THE PSF METHOD HAVE BEEN ADDED ACCORDING TO THE LEGEND.

The curve has been computed from the LSF method. Results for the PSF method have been superimposed on this curve. It is noticeable that the results for the MM of 5.1 mrad coincide with the curve. Assumptions on the linear behaviour of annuli with large MM's were therefore valid.

2.4.1(b) Low and Medium Contrast Targets.

The profiles obtained from the low and medium contrast targets were more complex than for the high contrast targets. As can be seen in fig.C5(a), for the very small annuli of 33 $\mu$rad and D=0.3, no maxima occurred. The profile is characterised by a dark central area corresponding with the MM, and no maxima above the background level. In this case the effect of the MM has completely blotted out the influence of the annulus. Other curves lie between the two extreme types of curves i.e. those with no maxima as described above, and those obtained from the simple high contrast targets.

Where significant maxima above background level occur in the convolution, corresponding percentage differences have been added to fig. 7. Each point is marked with its background density level. The following cases have been omitted from fig. 7 : D = 0.9 and 1.2, annulus = 6 $\mu$rad; differences in maxima were approximately $100^{o}/o$; D = 0.9, annulus = 33 $\mu$rad, difference = $80^{o}/o$; D = 0.3, annulus = 33 $\mu$rad and 63 $\mu$rad, no maxima occurred.

## 2.4.2 Slopes of the Profile.

Slopes of the intensity profile were determined from the profiles computed by the PSF method. No values were deduced from results computed from the LSF method. The position on the curves at which the slopes were calculated was the straight section on the main slope of the profile, where the rate of change in slope was a minimum. The reason for choosing this section is, if the visual system uses a slope in the intensity profile, it should be one which follows a simple pattern, and is of sufficient length to allow a good comparison of each side of the profile. It is believed that where rapid changes occur in the intensity profile, e.g. near the top of the profile, comparison of the slopes of the curve would present too difficult a problem for assessment by the visual system.

Differences in slopes when the MM is displaced by amounts equal to those in fig. 1, are presented in fig. 8, which expresses the percentage change in the slope of the profile in terms of annulus width. For the larger two measuring marks either side of each annulus profile gave approximately the same result. However, for the smaller MM, the inner flank of the profile was taken except for annulus widths of 50 and 100 $\mu$rad. For these two annulus widths the inner slopes are difficult to determine with any degree of accuracy because of their very limited length. In addition, it is felt that their length would be insufficient for the eye to discriminate differences in slope.

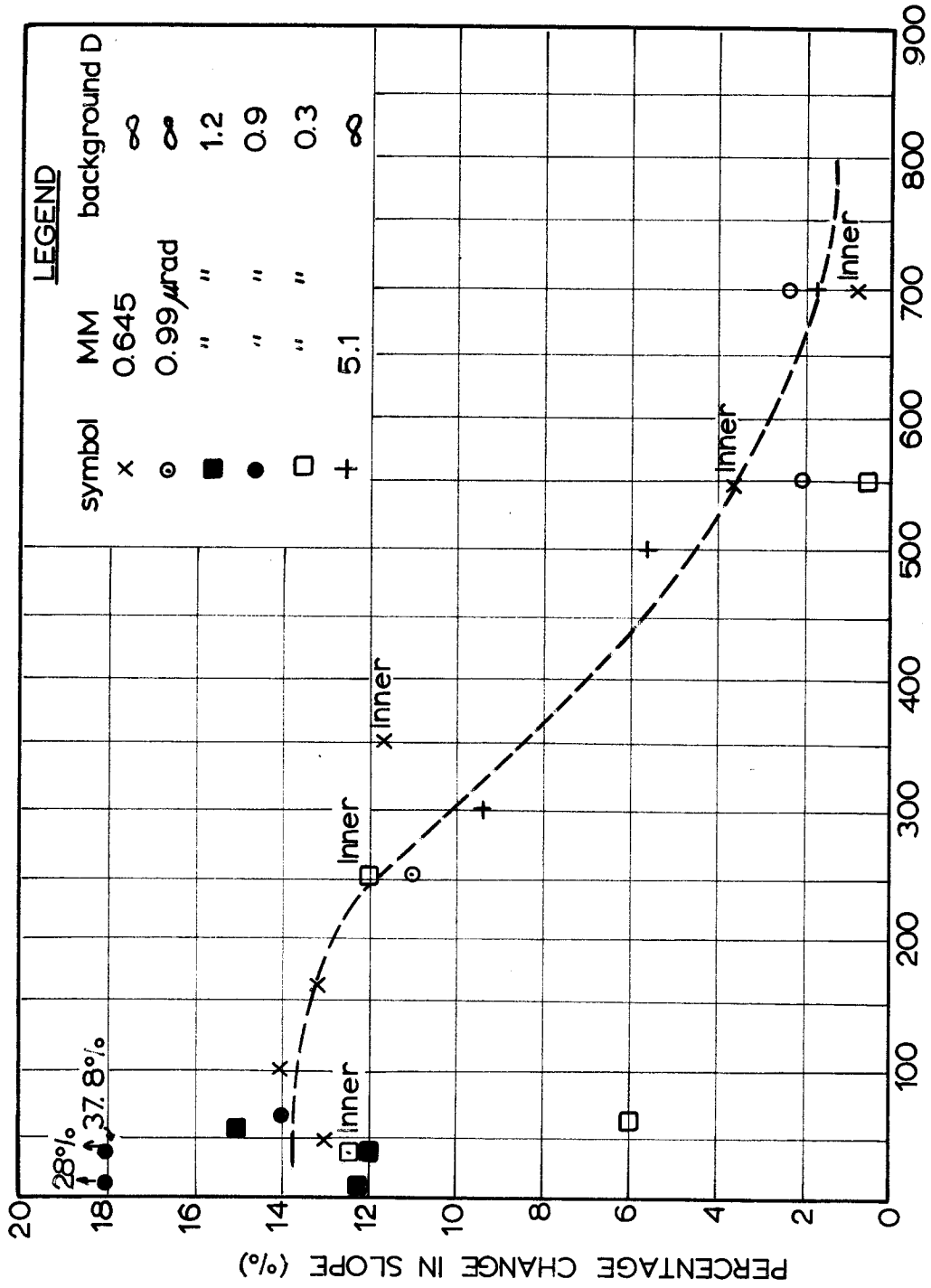


FIG. 8 THE RELATION BETWEEN THE VARIATION IN SLOPE OF THE INTENSITY PROFILES DERIVED BY THE PSF METHOD, AND ANNULUS WIDTH COMPUTED FROM POINTING ERRORS IN FIG. 1

For annulus widths greater than 100 $\mu$rad using 0.645 mrad MM, the inner slopes produce higher percentages than the outer slopes, and therefore were included in the graph. When inner slopes were used, the figure has been marked accordingly. The slopes of all curves for the low and medium contrast targets have also been added to Fig. 8.

The accuracy of slope determination, which is an average value over the approximately linear section of the curve, is about $1^{o}/o$. This is the section over which a determination of slope is most readily available. At this stage, analysis of slopes is in its preliminary stage, and therefore for an initial assessment it is felt that this method is satisfactory.

Despite slight inaccuracies of slope determinations, a general trend in the pattern of the percentage changes in slope is clearly visible in fig. 8, except for three values, which do not seem to follow any pattern. Maximum values range around $12\text{-}16^{o}/o$. for the annuli less than 200-250 $\mu$rad, after which values gradually decrease. The pattern is very similar to fig. 7. This similarity which is logical from geometrical point of view, will be referred in sec. 3, in relation to luminance discrimination by the visual system.

2.4.3 Widths of Luminance Profiles.

It has been pointed out in sec. 1.5 that the width of the target actually seen by the visual system can only be determined during the

observations. Since this has not been done for the data in hand, a choice of width was made at (1) the 60.6°/o luminance level, which is the level at which the 2σ-width is read on a purely gaussian curve and (2) the point of maximum slope. Although the latter criteria gave widths at luminance levels of 60.6°/o for purely gaussian curves, the widths were located at levels gradually decreasing for the non-gaussian curves, and tended towards the 50°/o level for a purely gaussian integral curve (the edge). These levels were computed in the previous work by the author. (See Appendix A.)

Indications are that these luminance levels may be too high. (Hempenius, 1966b). However, the experiments by Hempenius have not involved very small edges as in these experiments. It is also difficult to relate investigations on microscopic blurred edge determinations made by Watrasiewicz (1966) to the present blurred edges of small sharp targets. Two points however can be drawn from the investigations mentioned above. Width and edge determination depend on

(i) retinal illuminance, and

(ii) contrast of the object.

On viewing the relationship between the two criteria in fig. 9 however, it is felt that any errors will not significantly affect the conclusions.

If an error exists in the position of the MM, the annulus width seen by the visual system on one side of the MM will be larger, and on the

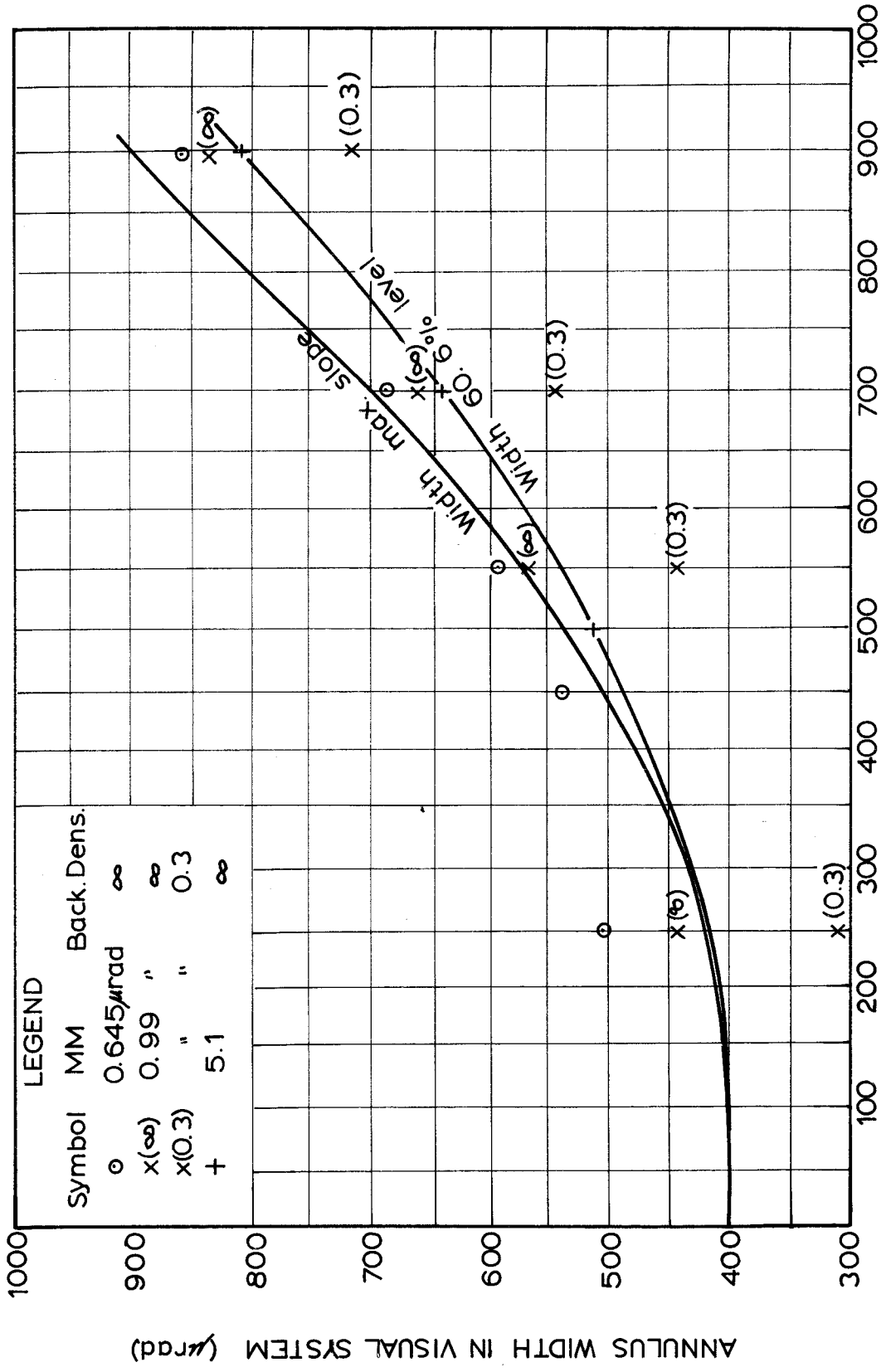


FIG. 9 RELATIONSHIP BETWEEN WIDTH IN OBJECT SPACE, AND WIDTH AS SEEN BY THE VISUAL, USING THE TWO CRITERIA FOR WIDTH, FOR CURVES DERIVED BY THE LSF METHOD. WIDTHS OF PROFILES AT 60.6% LEVEL, DETERMINED BY THE PSF METHOD HAVE BEEN ADDED, ACCORDING TO THE ABOVE LEGEND.

other, smaller than when the MM is correctly placed. The actual difference in widths of the two annuli is therefore twice the pointing error. To be consistent with the ratio defining Weber's Law, the total difference in annulus widths, seen by the visual system, which equals twice the error, must be equated to the sum of the widths of the annuli on each side of the MM. Alternatively, the effect in width on one annulus as seen by the visual system can be plotted against the original width of the annulus, since the changes on each side of the MM will be approximately equal.

Fig. 10 shows the curves representing those ratios using the two width criteria for LSF method. The ordinate scale is half the minimum visible difference in annulus width in the visual system, derived from pointing errors in fig. 1. On the abscissa scale is plotted the annulus width of the target in the visual system. The $1^{o}/o$-$2^{o}/o$ limits generally prescribed by Weber's Law have been added.

The differences in widths of the profiles caused by a displacement of the MM determined by the PSF method have been added to Fig. 10 at a number of points, for the $60.6^{o}/o$ intensity level only. The actual point at which the maximum slope occurs on each profile at this stage is unknown. Because of the curved nature of the annulus for small MM, the point of maximum slope will not be at the same level on profiles determined by the PSF method as for the LSF method. Further

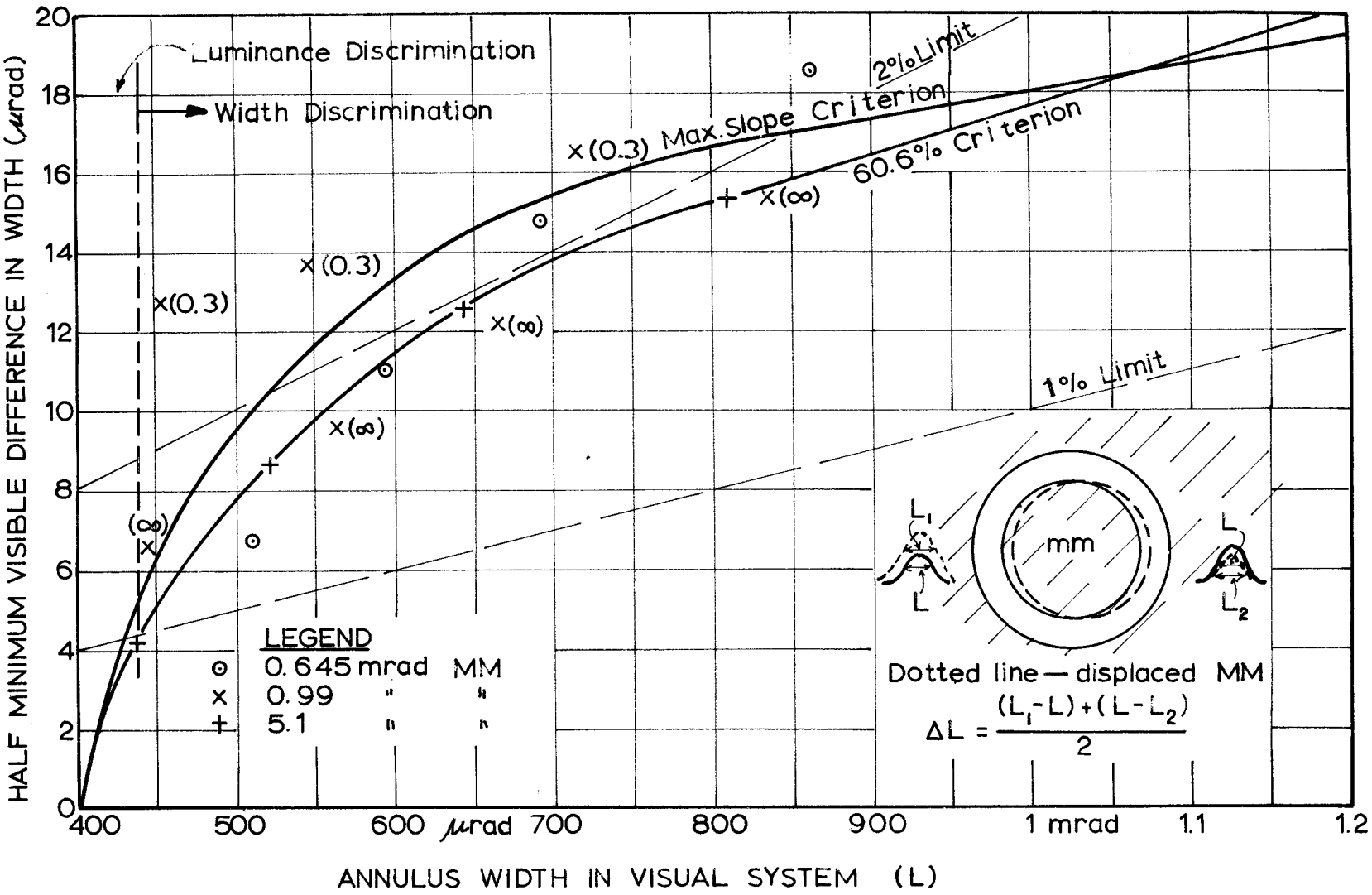


FIG. 10 THE RELATION, FOR IMAGE IN THE VISUAL SYSTEM, BETWEEN ANNULUS WIDTH L AND HALF THE MINIMUM VISIBLE DIFFERENCE IN ANNULUS WIDTH ΔL, DERIVED FROM POINTING ERRORS IN FIG. 1. THE COMPUTATIONS BY THE LSF METHOD GAVE THE TWO CURVES AS MARKED. COMPUTATIONS BASED ON THE PSF METHOD HAVE BEEN ADDED AND ANNOTATED ACCORDING TO THE LEGEND. RATIOS DEFINING WEBER'S HAVE BEEN ADDED.

investigation must be carried out to determine mathematically the point of maximum slope for all profiles.

Widths were interpolated linearly from the computed profile. Though this represents an approximation, no significant errors were introduced because the section of the curve at the 60.6°/o level is approximately linear. In addition, the good agreement obtained between the LSF method, and the PSF method using MM of 5.1 mrad in figs. 9 and 10, is further proof of this point. For the 0.99 mrad MM, the widths of the profiles were very close to those for the 5.1 mrad MM. Widths determined for the .645 mrad MM agreed with those obtained for the other two MM's, for larger annuli, but differed considerably for annuli less than approximately 400 μrad. This is mainly due to the tendency for the profiles of the small annuli to overlap.

Widths of the profiles of low contrast targets were less than those of high contrast targets. For instance, at 450 μrad, the width of the profile is only 400 μrad, and for smaller annuli, the width approaches zero, i.e. no maxima occur. The ratio of minimum visible difference in annulus width/width in visual system, ranges from 2.3°/o (derived from an annulus of 900 μrad) to 5.5°/o (derived from 250 μrad annulus - not plotted in fig. 10) and approaches infinity as annulus width approaches zero.

In general, the results in fig. 10 obtained for the LSF method agree well with those obtained by the PSF method for all MM's, and

even for the low contrast targets. The maximum annulus width computed by the PSF method was 900 μrad. Computation time for larger annuli becomes prohibitive. As there is a factor in computing time of about 100 between the two methods, the attitude adopted was to establish results by the LSF method, and then to carry out spot checks at various annulus widths, different MM's and background density by the PSF method. By this process, a very good estimate can be obtained of the relationship between widths of the convolved profiles, without consuming an excessive amount of computer time.

Based on figs. 8, 9 and 10, the significances of the shape of the luminance profile in the visual system and conclusions on the criteria for pointing can now be deduced.

## 3. DISCUSSION OF RESULTS OF CONVOLUTION.

### 3.1.1. Shape of Convolved Annulus.

The shape of the profile for a given annulus width depends mainly on the size of the MM. Direct comparison can be seen in the Appendix C. For the MM of 0.645 mrad, and annulus 42 μrad, the MM is almost completely obscured by the blurred profile of the annulus. This compares well with the results obtained by Gubisch (1967, 412). As the annulus becomes greater, the MM is more pronounced. (See figs. C2(a) and (b).) Whether the MM is in fact visible for annulus width of 42 μrad is not certain. The difference in luminance levels of the MM and annulus is 13.5°/o of the annulus maxima, for a centred

MM, and increases slightly to $15^{o}/o$ for the displaced MM. These values are lower than the estimated minimum visible differences prescribed in the following section. It is reasonable to assume therefore, that the MM for an annulus 42 $\mu$rad is not visible. Profile values show that the MM is probably visible for annulus widths of 100 $\mu$rad and greater for .645 mrad MM.

For larger MM, e.g. 0.99 mrad, the dark central area of the MM is clearly visible over the whole range of annuli. However, the fact that almost no central area exists in the profiles has little effect on the pointing accuracy, and each of the three profiles for annulus of 50 $\mu$rad gives almost the same accuracy. This agrees with conclusions reached by O'Connor, i.e. that the MM is of secondary importance in determing pointing accuracy. Stating these conclusions in terms of radiance profiles, the shape itself is of secondary importance in determing accuracies, but the effect on the profile when the MM is moved across the target is important. This effect, which is an imbalance between profiles on either side of the MM, is governed by the width of the annulus.

A general discussion on the shape of the curves for low and medium contrast targets has been given in sec. 2.4.1. Obviously the density background influences the shape of the profile considerably. In the case of small annulus widths, the luminance profile of the annulus is completely blotted out by the MM, thus reducing the profile to what seems to be a dark MM super-imposed on a uniform background. With

this type of profile comes a marked increase in pointing error.

It is apparent that the variations in maximum values, slopes and widths for a displacement of the MM, are a function of the geometry of the convolved curve. From figs. 7, 8 and 10, it is clear that variations in widths are the most prominent feature of curves derived from annulus widths greater than 250 $\mu$rad, while variations in slope and maxima are more prominent for annulus widths less than 250 $\mu$rad.

The results of the convolution can be applied to derive practical MM sizes for photogrammetric use. It is apparent if, for instance, the profile for 0.645 mrad MM, and 50 $\mu$rad annulus, were superimposed on a background of density 0.3, very large pointing errors would result. The MM is virtually obscured by the annulus spread in the high contrast case, and only small variations occur across the profile, at the position of the MM. Very large displacements of the MM would therefore be expected before significant variations in the annulus profile resulted. These variations must produce measurable differences in slope of the convolved annulus derived from the combination of annulus and MM profiles.

On the other hand, the MM of 0.99 mrad, the profiles of the two annuli virtually do not overlap, and therefore a more efficient situation exists for creating measurable differences in slope of a convolved annulus on a medium or low contrast background. From this point of view therefore a MM of 0.99 mrad would seem to be the smallest

practical size. O'Connor himself (1967, 73) has stated that this MM size is an ideal size for practical use in photogrammetry.

A discussion of pointing accuracy as a function of maxima, slopes and widths will follow.

### 3.1.2. Pointing Accuracy as a Function of Slopes and Maximum Values of the Radiance Profile.

Figs. 7 and 8 indicate the effects on maximum luminance values and slopes of the profile when the MM is displaced an amount equal to errors in fig. 1. For annulus widths less than at point B fig. 1, these curves are approximately constant at about 14-16°/o and 12-16°/o respectively. Above this level of annulus width the curves drop quickly. Apparently values of 14-16°/o and 12-16°/o are the minimum visible differences in maxima and slope of the intensity profile, and are therefore the criteria used for pointing between A-B. Width differences below point B are well below those prescribed by Weber's Law and therefore are not visible. Beyond point B, maxima and slope variations are less than the above values and therefore are assumed not visible.

On viewing the results from the low and medium contrast targets it is seen that for cases where no maxima occur, apparently only slope differences are used for pointing. It seems therefore, that differences in maxima are not a necessary criterion for pointing provided sufficient differences in slopes exist. One can postulate that if both are present, slightly more assistance is given to the

observer, and therefore higher pointing accuracy will result. Unfortunately, the accuracy of the slope determination is insufficient to check this. One could also question whether pointing is possible in a situation where differences in maxima of 14-16°/o but only very small differences in slope occurred. It appears, however, that slope variations with or without maxima variations, is the basic criterion used for pointing to targets in the range A-B. The three widely varying points in fig. 8 do not fit into the above pattern. At this stage no suitable explanation is available.

Slope discrimination would seem to be only an extension of the idea of luminance discrimination, i.e. instead of discrimination between values of luminances at two points on the profile, the observer discriminates between rates of change of luminance over corresponding sections of the profile. Hence slope is still within the bounds of the assumptions on basic discrimination capabilities of the visual system put forward in sec. 1.5.

The exact values of minimum visible differences of slope are not known. Whether the differences required for pointing are constant in all cases, or vary depending on features such as extent of sloped profile, magnitude of slope, adaptation level and general illumination conditions is a subject for further research.

In most investigations on visibility, research has concentrated on minimum visible differences in maxima rather than slope. The ratio

of minimum visible difference in luminance over field luminance is often termed Fechner's Fraction. The value for this fraction quoted by Walsh (1953, 62) and Graham (1965, 215) is 2°/o for 14 ml background luminance, and increases slightly to 3-4°/o as the effective background luminance drops, i.e. for annuli below point B fig. 1. To the best of the author's knowledge no similar figures are available for minimum visible differences in the slope of the radiance profile.

Röhler (1962) found by convolution, based on a slightly larger PSF, that the minimum visible difference in luminance profile when two dots were brought in close proximity with each other was 25°/o. The information given to the observers in each case, in the form of luminance profiles, is not the same, but their similarity is sufficient to substantiate the conclusions that values obtained for Fechner's fraction in this type of task, are much higher than values quoted above. The value of Fechner's fraction is greatly dependent on the particular viewing conditions, especially the angular field of view and adaptation level. Such factors could contribute to the much higher fractions encountered in these experiments, particularly considering the small size of annuli. It even seems likely that a slightly larger fraction may result for 50 μrad annuli, than for the 250 μrad annuli, and therefore the ratio between annulus width and pointing error in this range is not strictly linear. This appears to be the case in fig. 1. It also seems that similar reasons can explain the even larger fraction encountered by O'Connor in his observations in the dark adapted state, since adaptation level

influences the value of Fechner's fraction.

Whether the same deductions can be made on slope discrimination is a matter for conjecture. Determination of luminance profiles via spread functions is only a recently developed technique and therefore little opportunity has existed for full investigations on slope discrimination. In addition the problem is very specialized and therefore would not be treated by many scientists.

### 3.1.3. Pointing Accuracy as a Function of Width Discrimination for Larger Annuli.

Over the section B-C Fig. 1, the shape of the convolved curve undergoes a gradual transition from a height variation to width variation (beyond C). For annulus widths greater than at point B, errors as in fig. 1, cause changes in height and slope less than 14-16$^{o}$/o and 12-16$^{o}$/o respectively, which are unlikely to be visible. Apparently, luminance discrimination is not used as a criterion for pointing beyond B.

As pointed out in sec. 2.4.3. fig. 10 represents the relationship between annulus width in the visual system, and the corresponding effect on the annuli on each side of the MM, for a displacement of the MM equal to errors in fig. 1. This curve is actually section B-C fig. 1, plotted for the visual system. The differences between annuli on each side of the MM, which equal twice the errors in pointing, are the criteria used in pointing. Errors such as in fig. 1, represent the vernier acuity of the visual system but sensitivity is twice this amount. It follows then that errors in pointing equal half the minimum visible

difference in annulus width.

The ratio along the curves for high contrast targets in fig. 10 varies from approximately 1 to 2°/o for annulus widths greater than 427 μrad in the visual system derived by the LSF method, and the PSF method using 5.1 mrad MM. Below this width the ratio tends towards zero, and it is apparent that luminance discrimination rather than width discrimination is the criterion for pointing. The ratios are consistent with the 1-2°/o limits of Weber's Law, and it is therefore possible to relate Weber's Law to pointing over the range B-C, provided the widths are considered in the image space of the visual system.

The values determined by the PSF method superimposed on fig. 10 also generally lie within the limits of Weber's Law, although they do not exactly follow the curve determined by the LSF method.

Plotting fig. 10 on logarithmic scales makes the transformation from the object space to the image space clearer, i.e. fig. 11. The abscissa scale applies to the annulus width in object and image spaces, while the ordinate for the object space is the error in pointing (fig. 1), and for the image space, half the minimum visible difference in annulus widths, fig. 10. The limits of Weber's Law have been inserted and the arrows indicate the corresponding values after transformation. It is interesting to note that the abrupt change in the graph for the object space has been smoothed in the curve for the image space.

The choice of width of the spread function, can perhaps account for small anomalies in the results, but these have not been too great to

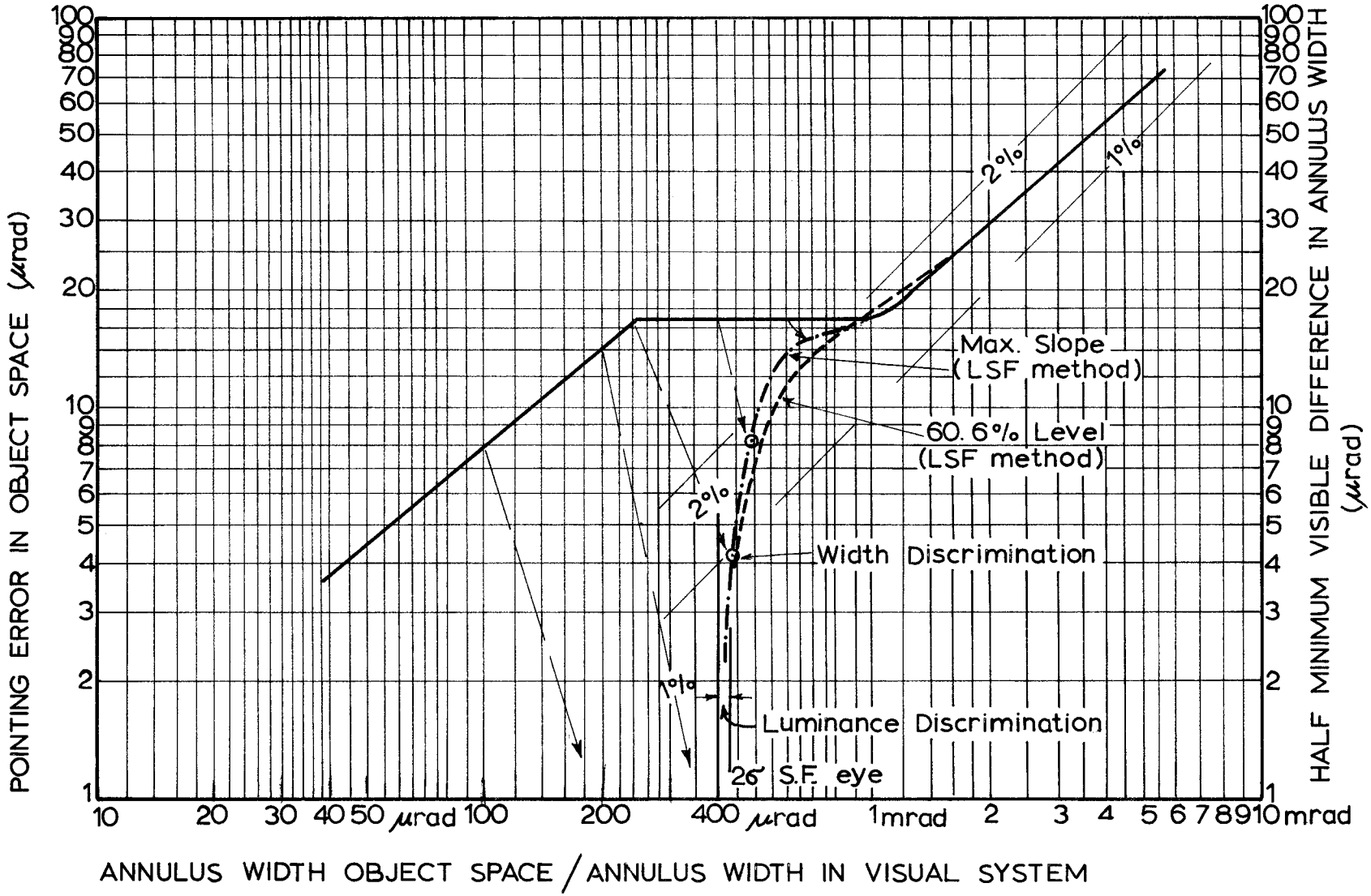


FIG. 11 THE TRANSFORMATION OF FIG. 1a, TRANSFORMING ANNULUS WIDTHS AND POINTING ERRORS MEASURED IN THE OBJECT SPACE, TO ANNULUS WIDTHS AND HALF THE MINIMUM VISIBLE DIFFERENCE IN ANNULUS WIDTH, AS SEEN BY THE VISUAL SYSTEM. THIS CURVE REPRESENTS THE RESULTS OBTAINED USING THE LSF METHOD.

obscure the reasoning. Despite variations in the position of the curves in fig. 10, the position of the transformed curve in fig. 11 is well defined.

Widths of the low contrast curves have been treated in the same manner. Determination of widths in these cases is more difficult particularly because of the asymmetry of the profile, but the criterion of 60.6°/o of the profile above background level was taken to determine the width. As mentioned in Sec. 2.4.3, the minimum visible differences in width for low contrasts generally were close to Weber's Law, although for smaller annuli the ratio gradually increased. Choice of width criterion may be a contributing factor in the larger values obtained. They are also dependent on the critical annulus width below which maxima of the profile above background become invisible to the observer. This is the annulus width at which slope discrimination becomes the criterion for pointing. The point at which width discrimination takes over from luminance discrimination for any MM or background density is impossible to predict with any degree of accuracy. Interpolating values from figs. 8, 9 and 10, this point occurs between 200 and 350 $\mu$rad, depending on the MM size and background density. Small discrepancies however do exist between the three figures. Without better criteria for width determination, more accurate estimates of the transition point are not available.

## 3.2 Discussion of Results Based on Dark Adaptation.

Errors in the observations under dark adaptation in fig. 1(b) were found to follow a steeper value below point B and the constant value between B and C was nearly 10 $\mu$rad higher than for the the other experiments.

Suggestions were made in sec. 3.1.2 that discrimination capabilities of slope and maxima may depend on viewing conditions. The section A-B when errors are approximately 10 $^{o}/_{o}$ of the annulus width substantiates this suggestion. For annulus widths greater than point B, it is possible that the different adaptation level may cause the observer to interpret the width at a level on the profile less efficient than the level used for the normal experiments. Experiments by Watrasiewicz (1966) on edge location of microscope targets confirm this tendency, that the subject edge location is a function of retinal illuminance.

## 4. SUMMARY.

With regard to the choice of physiological data on the eye, three points can be drawn from the previous section:-

(i) The choice of the two criteria for width determination, has not led to any gross differences between the two curves in fig. 11. It is felt that the actual level used by the observer will not differ significantly from these two positions, and therefore the correct position of curves in fig. 11 will not vary greatly from that determined.

(ii) A value of 400 μrad for the SF of the visual system has proved generally suitable. However, on viewing fig. 8 it seems that an annulus width of approx. 200 μrad is the point at which width discrimination takes over, whereas in fig. 1, the change is at approximately 240 μrad to 300 μrad depending on MM size. The SF used could therefore be slightly too small. On the other hand minimum visible differences in slope and maxima may decrease slightly as the annulus width increases.

(iii) As stated by O'Connor (1962), Weber's Law has been applied to problems of discrimination, with the proviso that the objects are not too large or too small. Objects too large have not been observed even in O'Connor's first study. However, Weber's Law has been proved applicable to small targets down to approximately 250 μrad in object space, provided widths are measured on the image seen by the visual system. The provision of "not too small" can be restated for pointing to sharp targets based on the two width criteria in this paper, as "provided the width of annulus in the visual system is greater than approximately 440 μrad." Small variations in this limiting point may result for different background densities. Above this width, a movement of the MM by 1-2$^{o}$/o of the annulus width in the visual system introduces a visible

variation in the widths; below this width, observation of differences in widths proves less efficient than viewing differences in slope and maxima of the luminance profile, and therefore Weber's Law no longer applies.

## 5. FURTHER APPLICATION.

The targets used to derive fig. 1 are not those normally encountered in photogrammetry. This is for two reasons:

(i) annuli encountered in photogrammetry rarely go below point B, (Point B corresponds with a MM of 15 $\mu$m on a target of 30 $\mu$m at 10 x magnification).

(ii) image qualities of photogrammetric targets are not normally as good as those used for the present investigations.

However, similar procedures can be applied to pointing accuracies for photogrammetric targets as were used in the foregoing procedure. The irregularly shaped annuli between the sharp MM, and the blurred target will require more complex convolution procedures. It is believed that the criteria derived in Sec. 3 will be applicable to such blurred targets.

## 6. CONCLUSIONS.

1. The approach of determining the shape of annulus in the visual system proved successful in explaining pointing accuracies to small targets.

2. Parallel to the findings of O'Connor[5], the shape of the luminance

profile is of secondary importance in determining pointing accuracy, but the effect on the profile of small movements of the MM is important.

3. Differences in widths between opposite sides of the annulus of both high and low contrast targets, are visible if they exceed approximately 1-2$^{o}$/o of the sum of annulus widths provided these widths are measured in the visual image. This applies to annulus widths greater than approximately half the 2$\sigma$-width of the spread function of the visual system.

4. Pointing to targets with annulus widths less than a half the 2$\sigma$-width of the spread function of the visual system, is based on discrimination of slopes and perhaps maximum values of the luminance profile. For the experiments described the minimum visible differences in slopes of approximately 12-16$^{o}$/o and in maximum values of 14-16$^{o}$/o resulted in pointing accuracies of approximately 8$^{o}$/o of the annulus width.

5. Pointing criteria as outlined in 3 and 4 above depend on the observation conditions, and therefore may vary for different experiments.

## APPENDIX A.

In the convolution of the line element and the LSF, the intensity levels for the point of maximum slope will be given for two extreme cases. The intensity level for the point of maximum slope using any other line element widths, will lie between these two extreme values.

The basic formula for convolution is -

$$h(x) = \int_{-\infty}^{+\infty} f(x-z)g(z)dz \qquad \ldots\ldots\ldots\ldots (A1)$$

where $f(x) = \exp -\frac{1}{2}(x^2/\sigma^2)$

$g(z) = 1 \qquad -c < z < +c$

$= 0 \qquad -c > z > +c$

where $2c$ = width of annulus

$$\therefore \quad h(x) = \int_{-c}^{+c} \exp\left\{-\tfrac{1}{2}(x-z)^2/\sigma^2\right\} .1.dz \qquad \ldots\ldots\ldots\ldots (A2)$$

(i) If 2c is infinitely small, the above expression reduces to the function

$$h(x) = \exp\left\{-\tfrac{1}{2}(x^2/\sigma^2)\right\}$$

i.e. the gaussian or error curve.

The point of maximum slope on this curve is given by the 1st derivative

i.e. $x_{\text{max slope}} = \pm \sigma$

On substitution of this value for x

$$h(x) = 0.606h(x)_{\text{max.}}$$

This result applies to the case of an infinitely fine line spread by the LSF. By definition this in fact gives the LSF.

(ii) If $2c \rightarrow \infty$

If the width of the annulus approaches infinity, the annulus is so wide that only one edge of the annulus is seen by the observer at any one time. Hence the observer will see an "edge" intensity profile, being a graded change in the profile from dark to bright.

No mathematical solution exists for the integral of the gaussian curve. However, the integral is tabulated in a number of texts on statistics. Solution of the equation A2 can therefore be carried out using these tables.

The point of maximum slope occurs at the $50^{o}/o$ intensity level for the edge profile, while $\sigma$-widths are located at $84^{o}/o$ and $16^{o}/o$ intensity levels. See fig. A1.

(iii) For cases in which $0<2c<\infty$, the points of maximum slope move gradually from $60.6^{o}/o$ level as in case (i) to the $50^{o}/o$ level in case (ii) as 2c increases.

A plot of this relationship is given in (Trinder, 1965, 80).

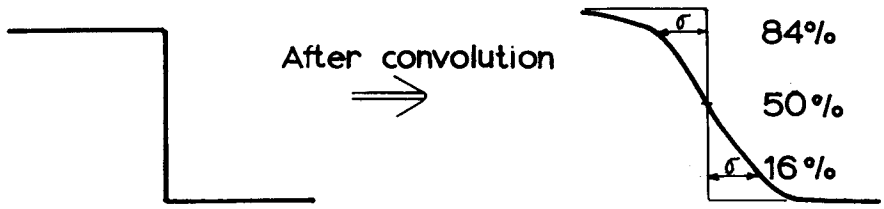


FIG. A1 EDGE PROFILE

## APPENDIX B.

The Density (D) of a material is given by the formula

$$D = \log_{10}\left(\frac{I_o}{I}\right)$$ ; where $I_o$ is the incident intensity, and I is the transmitted intensity.

Therefore, if **D** = 0.3, incident intensity is twice transmitted intensity. That is, background intensity will be 18.5 mL, if incident luminance is 37 mL. Similar computations can be

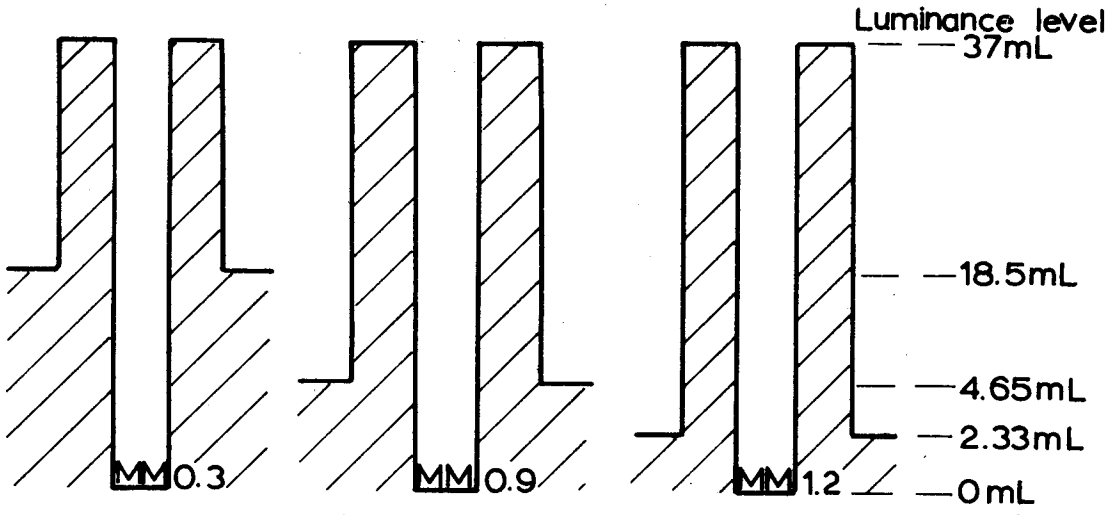


Target Density

Fig. B1.

Cross-Sections of the Luminance profiles of the measuring mark and target combinations for the three background density levels used in the experiments i.e. 0.3, 0.9, 1.2

carried out for the densities of 0.9 and 1.2 See fig. B1.

In the convolution of these profiles, the influence of the section below the background level, i.e. MM, must be weighted against the annulus profile above background. For instance, the annulus and measuring

mark profiles were given equal weight for the density of 0.3, because the luminance intensities above and below background are equal. For the densities of 0.9 and 1.2, weighting was 7.15 to 1 and 14.9 to 1 respectively, for annulus to MM influences.

# APPENDIX C.

Luminance profiles determined by the PSF method (see text), together with corresponding luminance profiles before convolution. The units for height of the profiles after convolution are arbitrary, but have been drawn to a consistent scale on each page. In the luminance profile before convolution, the heights have been decreased for reasons of space.

MM 5.1 mrad
HIGH CONTRAST

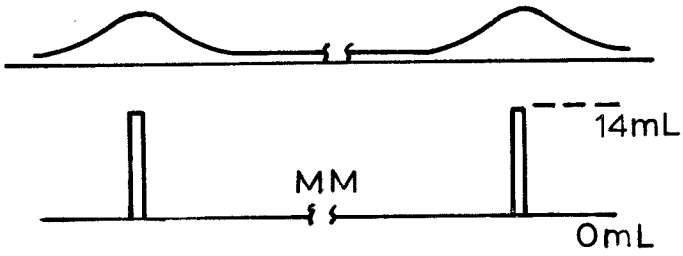




(a) Target diameter 5.2 mrad
Annulus = 50 μrad

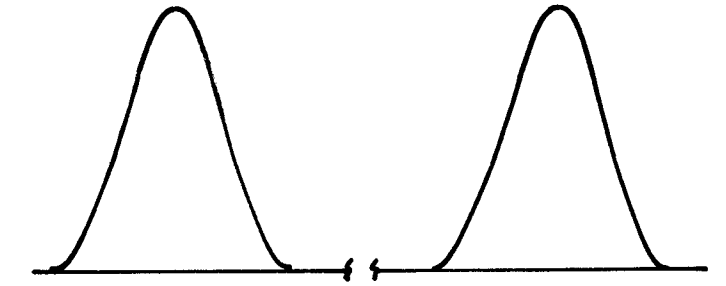




(b) Target 5.7 mrad
Annulus 300 μrad

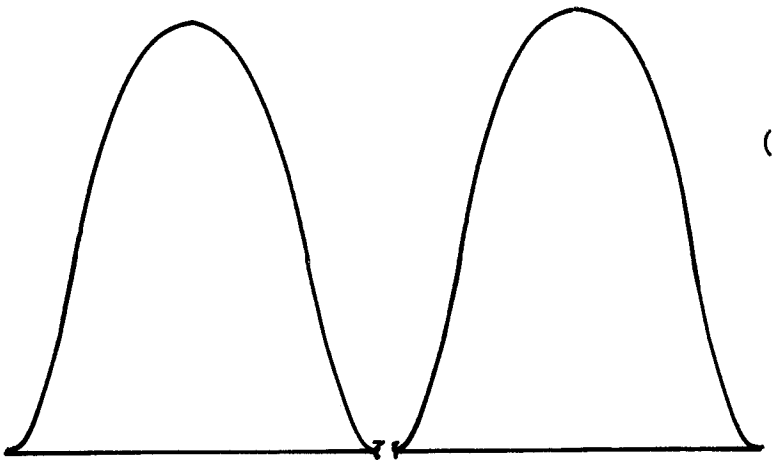




(c) Annulus 700 μrad
Target 6.5 mrad

FIG. C1

MM 0.645 mrad
HIGH CONTRAST

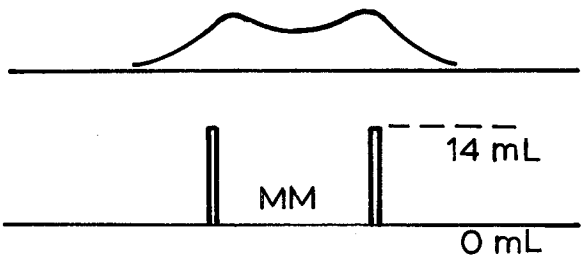


(a) Target 655 mrad
Annulus 50 μrad

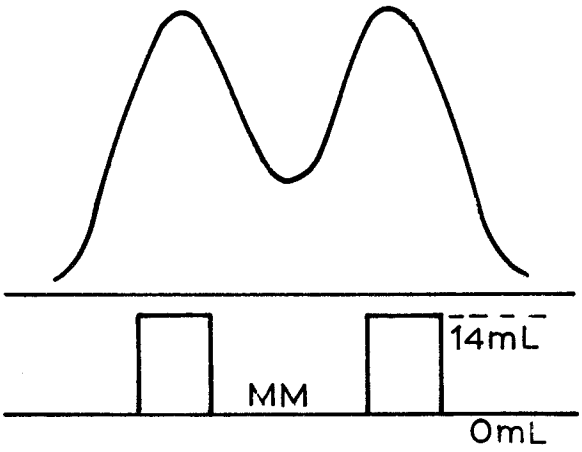


(b) Target 1.245 mrad
Annulus 300 μrad

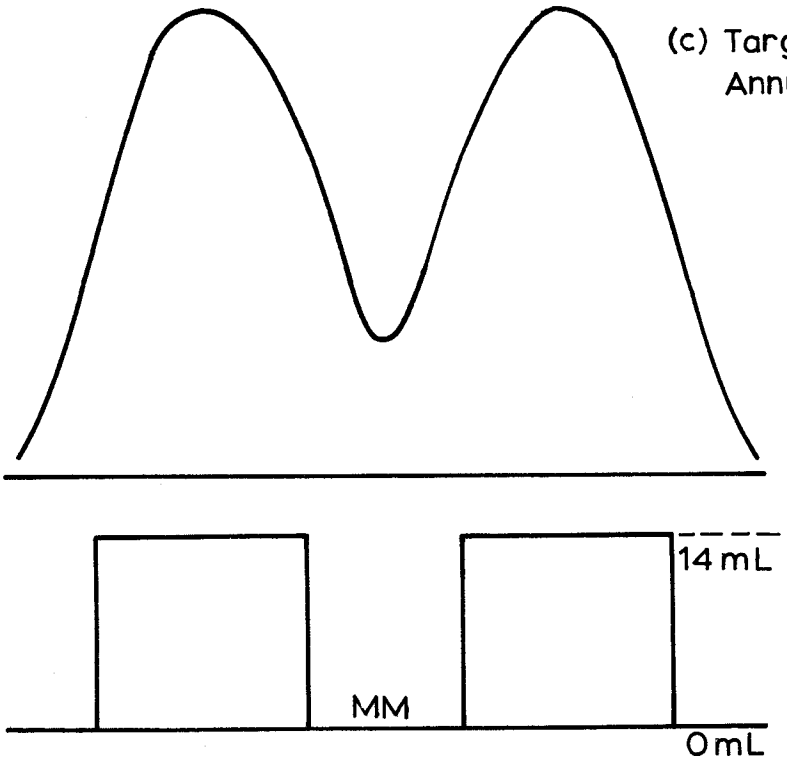


(c) Target 2.445 mrad
Annulus 900 μrad

FIG. C2

# MM 0.99 mrad
# HIGH CONTRAST

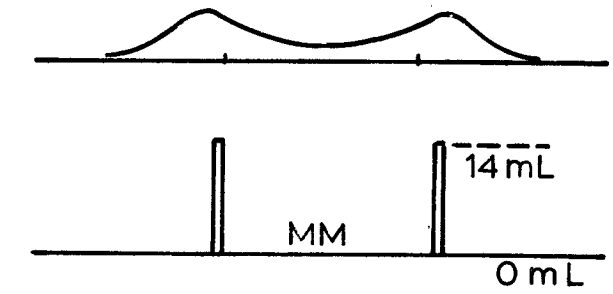

(a) Annulus 50 μrad
Target 1.09 mrad




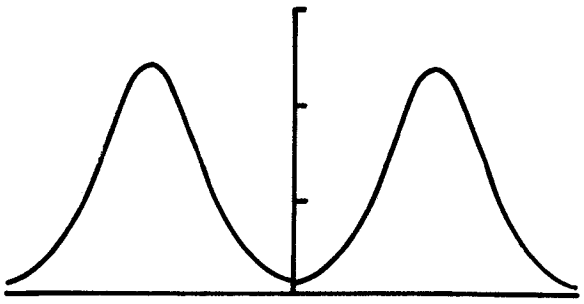

(b) Annulus 250 μrad
Target 1.99 mrad

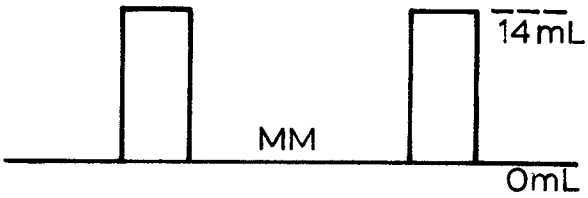


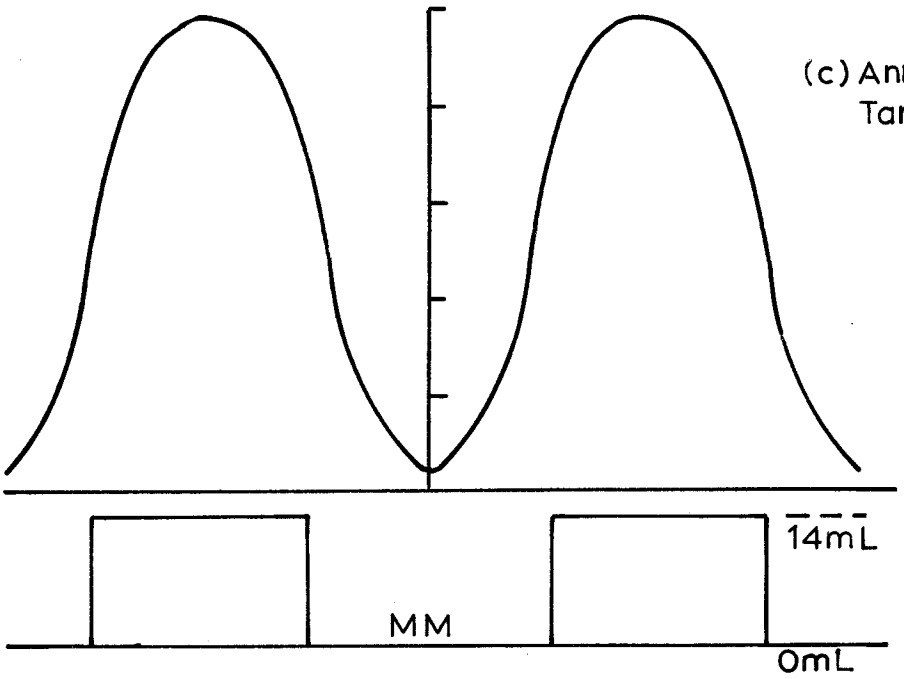

(c) Annulus 900 μrad
Target 2.79 mrad



FIG. C3

# MM 0.99 mrad
# MEDIUM CONTRAST

(a) Annulus 6 μrad
Target 1.002 mrad
D = 1.2

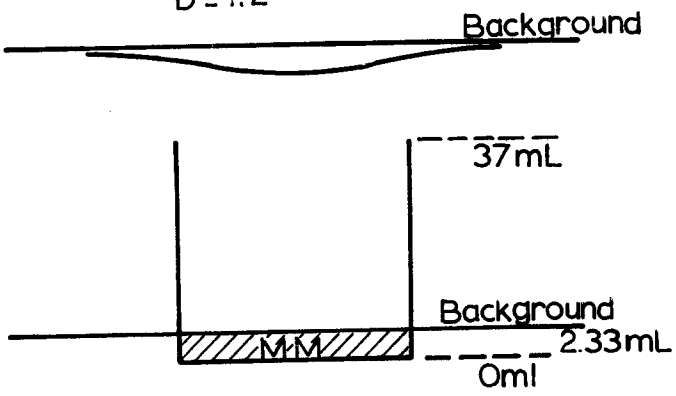


(b) Annulus 33 μrad
Target 1.056 mrad
D = 1.2

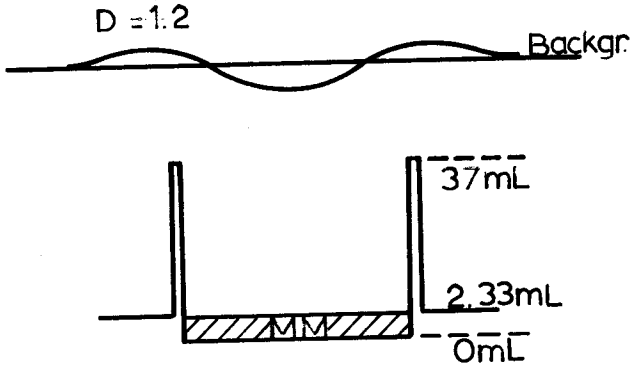


(c) Annulus 63 μrad
Target 1.116 mrad
D=1.2

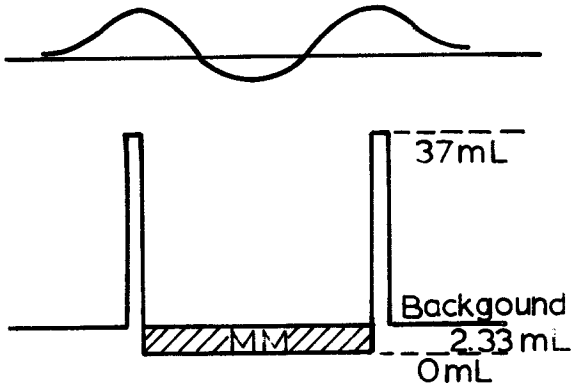


(d) Annulus 6 μrad
Target 1.002 mrad
D=0.9

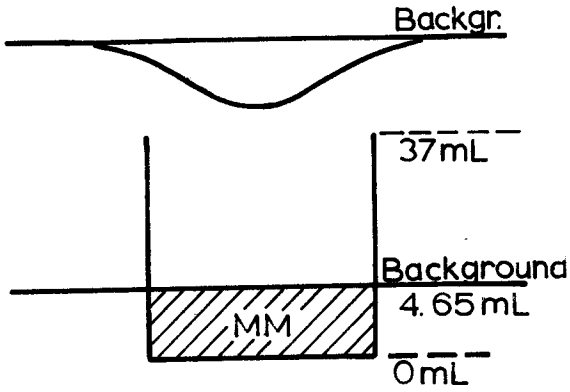


(e) Annulus 63 μrad
Target 1.056 mrad
D=0.9

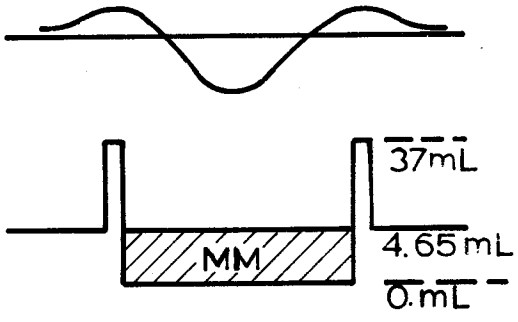


FIG. C4

MM 0.99 mrad
LOW CONTRAST

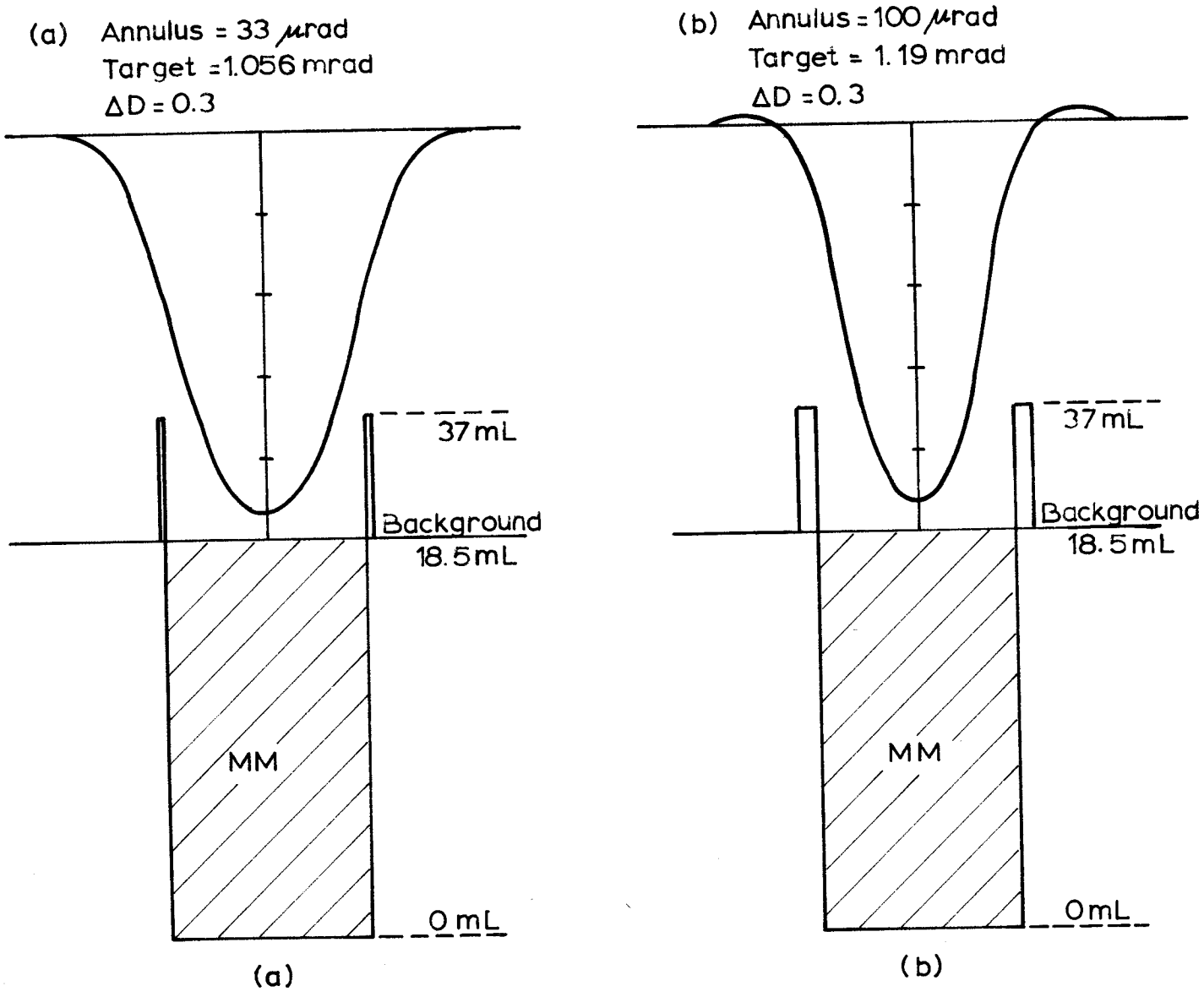


FIG. C5

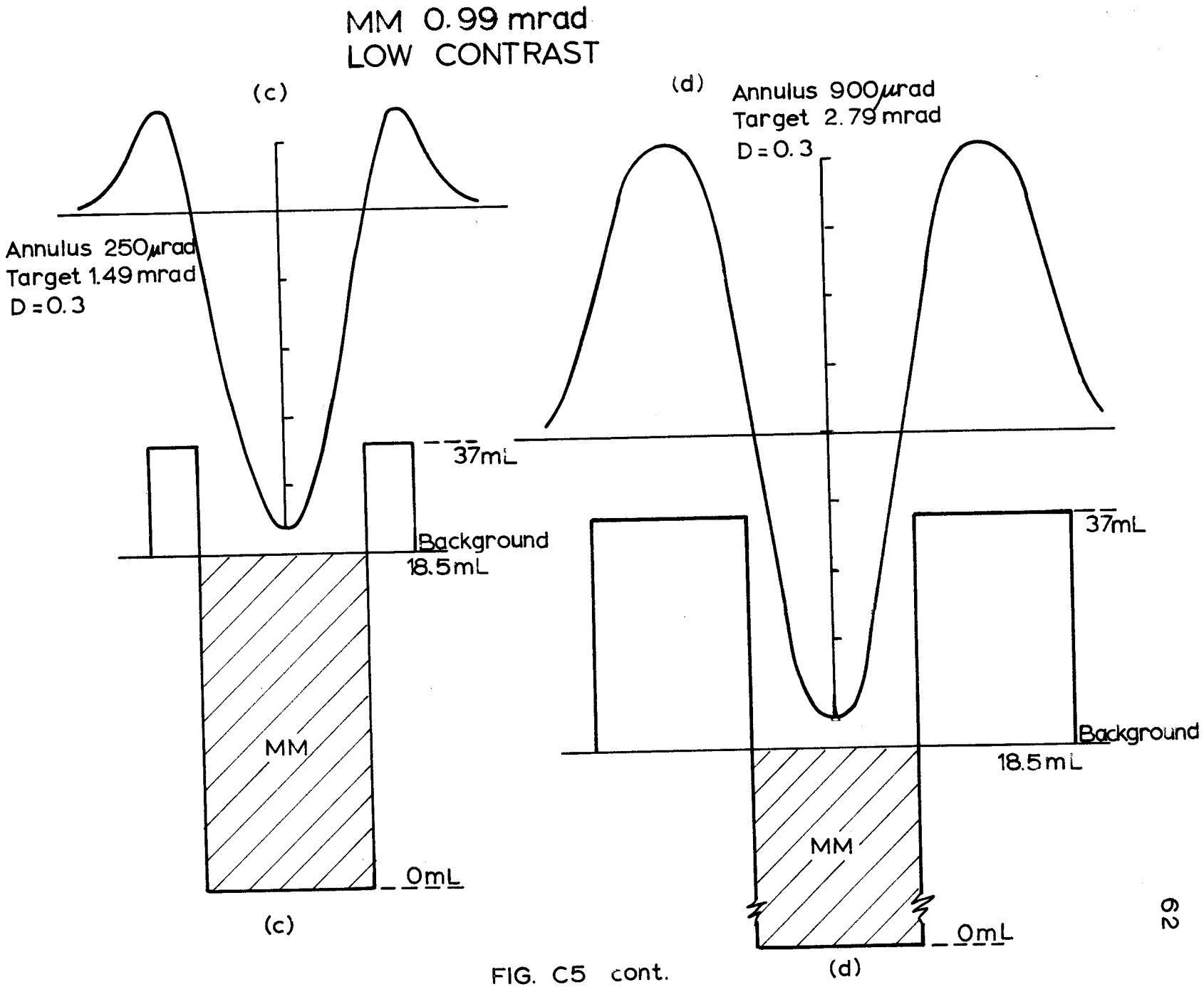
MM 0.99 mrad
LOW CONTRAST
(c)
Annulus 250μrad
Target 1.49 mrad
D = 0.3
37mL
Background
18.5mL
MM
0mL
(c)
(d)
Annulus 900μrad
Target 2.79 mrad
D = 0.3
37mL
Background
18.5mL
MM
0mL
(d)

FIG. C5 cont.

REFERENCES.

BOYNTON, R.M. "Progress in Physiological Optics", Applied Optics, 1967. 6, 1283-1293.

CHARMAN, W.W. and WATRASIEWICZ, B.M. "Mach Effect Associated 1964. with Microscopic Images", J. Opt. Soc. Am., 54, 791-795.

FRY, G.A. Letter, J. Opt. Soc. Am., 55, 333. 1965.

GRAHAM, C.H. - Editor. "Vision and Visual Perception", Publ. 1965. John Wiley and Son, New York.

GUBISCH, R.W. "Optical Performance of the Human Eye". J. Opt. 1967. Soc. Am., 57, 407-415.

HEMPENIUS, S.A. "Physical Investigations on Pricked Points Used 1964. in Aerial Triangulation", Photogrammetria, 19, 301-328.

HEMPENIUS, S.A. "Spread Functions and Transfer Functions in Image 1965. Formation, and Image Recording", I.T.C. - Lecture Notes.

HEMPENIUS, S.A. et al, "Logical Thoughts on the Psychology of 1966a. Photo-Interpretation", I.S.P. Commission VII C.I.P. Congress, Paris.

HEMPENIUS, S.A. "Applications of Image Quality Data and Theory 1966b. in Photogrammetric Research and Practice", I.S.P. Commission I Symposium, London.

JENNISON, R.C. "Fourier Transforms and Convolution for the 1961. Experimentalist," Pergamon Press London.

KRAUSKOPF, J. "Light Distribution in Human Retinal Images," 1962. J. Opt. Soc. of Am., 52, 1046.

LOWRY, E.M. and DE PALMA, J.J. "Sine-Wave Response of the 1961. Visual System I. The Mach Phenomena," J. Opt. Soc. Am., 51, 740-746.

O'CONNOR, D.C. "On pointing and Viewing to Photogrammetric 1962. Signals," I.T.C. Publication A 14/15.

O'CONNOR, D.C. "Visual Factors Affecting the Precision of 1967. Coordinate Measurements in Aero Triangulation," University of Illinois, Civil Engineering Studies, Photogrammetric Series No. 6.

PATEL, A.S. 1966. "Spatial Resolution by Human Visual System. The Effect of Mean Retinal Illuminance," J. Opt. Soc. Am. 56, 689-694.

RATLIFF, F. 1965. "Mach Bands: Quantitative Studies on Neural Networks in the Retina," Holden-Day Inc., San Francisco.

RÖHLER, R. 1962. "Die Abbildungseigenschaften der Augenmediem," Vision Research, 2.

SCHMID, H.H. 1964. "Analytical Photogrammetric Instruments," Photogrammetric Eng., XXX, 4, 559-567.

TRINDER, J.C. 1965. "Retinal Image Criteria in Photogrammetric Rinting," M.Sc. Thesis I.T.C. Delft.

WATRASIEWICZ, B.M. 1966. "Some Factors Affecting the Appearance of Mach Bands," J. Opt. Soc. Am., 56, 499-503.

WALSH, J.W.T. 1953. "Photometry," Constable and Co. Ltd., London.

WESTHEIMER, G. and CAMPBELL, F.W. 1962. "Light Distribution in the Image formed by the Living Human Eye," J. Opt. Soc. Am. 52, 1040-1045.

## BIOGRAPHICAL NOTES.

JOHN TRINDER graduated from the University of New South Wales with a Bachelor's degree in Surveying in 1963. He then spent two years at the International Training Centre at Delft, Holland, where he specialised in Photogrammetric Engineering and received both a bachelor's and a master's degree. Mr. Trinder has practiced as a Surveyor in New South Wales from 1960 to 1963 and joined the staff of the University of New South Wales in 1965 where he now holds the position of Lecturer.

Mr. Trinder has carried out research into the determination of monocular pointing criteria as a function of the shape of the retina image. His current research interests are the physiology of vision as applied to monocular and stereoscopic pointing in photogrammetry, and the assessment of image quality of aerial photography.

DEPARTMENT OF SURVEYING - UNIVERSITY OF NEW SOUTH WALES

Kensington, N.S.W. 2033.

Reports from the Department of Surveying, School of Civil Engineering.

1. The discrimination of radio time signals in Australia.
   G.G. BENNETT (UNICIV Report No. D-1)

2. A comparator for the accurate measurement of differential barometric pressure.
   J.S. ALLMAN (UNICIV Report No. D-3)

3. The establishment of geodetic gravity networks in South Australia.
   R.S. MATHER (UNICIV Report No. R-17)

4. The extension of the gravity field in South Australia.
   R.S. MATHER (UNICIV Report No. R-19)

UNISURV REPORTS.

5. An analysis of the reliability of Barometric elevations.
   J.S. ALLMAN (UNISURV Report No. 5)

6. The free air geoid in South Australia and its relation to the equipotential surfaces of the earth's gravitational field.
   R.S. MATHER (UNISURV Report No. 6)

7. Control for Mapping. (Proceedings of Conference, May 1967).
   P.V. ANGUS-LEPPAN, Editor. (UNISURV Report No. 7)

8. The teaching of field astronomy.
   G.G.BENNETT and J.G.FREISLICH (UNISURV Report No. 8)

9. Photogrammetric pointing accuracy as a function of properties of the visual image.
   J.C. TRINDER (UNISURV Report No. 9)

10. An experimental determination of refraction over an Icefield.
    P.V. ANGUS-LEPPAN (UNISURV Report No. 10)